

# Potential effects of electromagnetic fields in the Dutch North Sea

Phase 2 – Pilot field study

**Client:**

Rijkswaterstaat

**Date**

31-01-2020

**Clients Reference:**

31139799

**Our Reference:**

WP2018\_1130\_R3r3

**Version:**

Final



**Bureau Waardenburg**  
Ecology & landscape

## Title

Potential effects of electromagnetic fields in the Dutch North Sea. Phase 2 – Pilot field study

## Client

Rijkswaterstaat

## Reference

WP2018\_1130\_R3r3

## Keywords

Electromagnetic fields, EMF, impact, OWF, power cable, North Sea.

## Summary

A desk study on potential effects of subsea cables on species in the North Sea (Snoek et al. 2016), showed field measurements of EMFs are scarce. This report presents the results of EMF field measurements carried out in 2019 as well as the results from the video observations of mobile megafauna simultaneously recorded and an update of international scientific literature regarding EMFs and effects on marine life (in the North sea).

The developed methodology consisting of a measurement sledge equipped with real-time EMF measurements in combination with video recordings, has proven to be a valuable method to accurately determine the cable, measure EMF values and make recordings of the marine life above and in the vicinity of the cables. There are still operational limitations with respect to wave height that needs to be improved in order to be able to measure under maximum power production conditions as well.

Measured EMF values are relatively low, since measurements are conducted during low wind speeds only due to operational limits. Still, EMF values are in the same range in comparison to measurements at OWF export cables in Belgium.

The collected dataset was - due to the mentioned operational limits - too limited to be used for model validation.

Based on a single observation, for at least two species groups a difference in density directly above the cable compared to areas further away was observed. Considering that this is only a single observation and no repeated quantitative research and analysis could be conducted, no firm conclusions could be drawn from the results of this field study.

This study shows demonstrates the feasibility of conducting EMF measurements in combination with camera observations above offshore OWF export cables and forms a solid basis for future research aiming at a more quantitative assessment of both EMF values and impact on marine life.

## Acknowledgements

We would like to thank Maarten de Jong, Martine Graafland and Sarah Marx for careful reading of the draft report and helpful comments and suggestions. We would like to thank Helga van der Jagt for technical assistance in the field. Furthermore, we would like to thank Sytske van den Akker (Eneco) and Roos Knulst (Noordzeewind) for providing recent survey data of the export cables and wind farm production data during the measurements of the wind park Luchterduinen, Prinses Amaliawindpark and wind park Egmond aan Zee.



Version	Date	Author	Review & Approval
R3r0	31-08-2019	R.C. Snoek	L.M. Perk W. Lengkeek
R3r1	01-10-2019	C. Böhm	
R3r2	23-01-2020	K. Didden	
R3r3	31-01-2020	W. Lengkeek F.M.F. Driessen M.A.M. Maathuis	



# TABLE OF CONTENTS

<b>Table of contents</b> .....	<b>4</b>
<b>1 Introduction</b> .....	<b>6</b>
1.1 Background.....	6
1.2 Objective.....	6
1.3 Report outline.....	7
<b>2 Methodology</b> .....	<b>8</b>
2.1 Introduction.....	8
2.2 Wind conditions & production data during measurements.....	8
2.3 Study area.....	10
2.3.1 Cable burial.....	10
2.3.2 Measurement locations.....	12
2.4 Equipment.....	15
2.4.1 Set up.....	15
2.4.2 EMF-instrument.....	16
2.4.3 Underwater camera system.....	17
2.4.4 Synchronizing camera and EMF sensors.....	18
2.5 Survey vessel Bumblebee.....	18
2.6 Analysis.....	19
2.6.1 EMF measurements.....	19
2.6.2 EMF calculations.....	19
2.6.3 Camera footage.....	20
<b>3 Results EMF's</b> .....	<b>22</b>
3.1 Beach pilot 2018.....	22
3.2 Offshore EMF field values.....	23
3.2.1 Luchterduin (LUD).....	23
3.2.2 PAWP.....	23
3.2.3 OWEZ.....	25
3.1 EMF-values vs. Power.....	26
3.2 (Potential) Impact zone.....	27
<b>4 Results Marine Life</b> .....	<b>29</b>
4.1 Field pilot.....	29
4.1.1 PAWP cable (04-06-2019).....	29



4.1.2	LUD cable (20-06-2019) .....	31
4.1.3	PAWP cable (20-06-2019) .....	33
4.1.4	OWEZ cable (20-06-2019) .....	35
4.1.5	Biodiversity in relation to EMF strength.....	38
<b>4.2</b>	<b>Literature review.....</b>	<b>39</b>
4.2.1	Desk study on the potential impacts of EMFs on marine ecosystems .....	39
4.2.2	EMF literature 2017-2019 .....	40
<b>5</b>	<b>Conclusion .....</b>	<b>44</b>
<b>5.1</b>	<b>Methodology .....</b>	<b>44</b>
<b>5.2</b>	<b>EMF Measurements .....</b>	<b>44</b>
<b>5.3</b>	<b>Marine Life .....</b>	<b>45</b>
<b>6</b>	<b>Discussion .....</b>	<b>46</b>
<b>6.1</b>	<b>Measurements of EMF's .....</b>	<b>46</b>
<b>6.2</b>	<b>Marine Life .....</b>	<b>46</b>
<b>6.3</b>	<b>Current knowledge on potential impact of EMFs .....</b>	<b>47</b>
<b>6.4</b>	<b>Recommendations.....</b>	<b>48</b>
<b>7</b>	<b>References.....</b>	<b>49</b>
	<b>Appendix A.....</b>	<b>51</b>
	<b>A1. Cable types .....</b>	<b>51</b>
	<b>Appendix B Calibration certificate.....</b>	<b>52</b>

# 1 INTRODUCTION

## 1.1 BACKGROUND

A strong increase in development of offshore wind farms (OWFs) in the Dutch coastal zone is foreseen in the coming years. Besides the existing farms at Offshore Windpark Egmond aan Zee (OWEZ), Prinses Amalia Wind Park (PAWP), Luchterduinen and Gemini, the wind farm areas Borssele, Hollandse Kust Zuid and Hollandse Kust Noord will be developed. The produced power by the wind turbines will be transported in the wind farm by infield cables towards the transformer station, from which it will be transported to shore by export cable(s).

Wind parks in the Dutch North Sea are currently connected with alternating current (hereafter referred to as AC) cables to shore. In the future, for OWFs at larger distances from shore, export cables using direct currents (hereafter referred to as DC) are expected to be used as well.

The subsea power cables are known to induce electric fields (EF) and therefore generate electromagnetic fields (EMF). The strength of the induced fields depends on several aspects, but mainly on current intensity (which in turn depends on wind strength), type of cable, distance from cable (burial depth) as well as type of current (AC vs DC).

Higher electrical currents in subsea power cables are expected in future. This is because (1) an expected larger capacity of individual wind turbines (infield cables), (2) the scaling-up of wind parks, (3) the use of one single export cable to shore for several combined offshore wind parks.

The impact of these electromagnetic fields on the marine ecosystem is largely unknown. Limited available literature indicates possible disturbance or avoidance at the cables by certain species. However, data and knowledge about the impact on species that are specifically present in the Dutch North Sea is lacking.

Currently, a number of power cables are present perpendicular to the coastline, which in theory may form a barrier for species. The development of new OWFs and new export cables to Offshore High Voltage Stations (OHVS) can increase the chance of potential impact on these species.

In 2016, WaterProof Marine Consultancy & Services BV (WaterProof) and Bureau Waardenburg (BuWa) conducted a desk study to summarize the potential effects of undersea cables on species in the North Sea (Snoek et al. 2016). One of the main recommendations of the conducted study was to validate *in situ* the model results of EMF, generated by undersea infield- and export cables. Therefore, WaterProof and BuWa conducted EMF measurements in June 2019 in combination with video observations just above several subsea export cables offshore. This was done for the export cables of LUD, PAWP as well as the three export cables of OWEZ. Also, an update of international scientific literature regarding EMFs and effects on marine life (focused on the North sea) was made.

## 1.2 OBJECTIVE

The overall objective of the project is to increase our understanding of EMFs and related effects on marine species by offshore wind power cables in the North sea. The aim is to collect field data in and around export cables of 1) EMF field values and compare these with model values and of 2) the behaviour and occurrence of mobile megafauna.

## 1.3 REPORT OUTLINE

This report presents an overview of the conducted measurements and video observations above several undersea export cables in the Dutch North Sea.

Chapter 2 describes the methodology, such as study area, instruments and data analyses. In Chapter 3 and Chapter 4 the results of the EMF measurements and the marine macrofauna observations based on the field campaigns are given. In chapter 4, also an update of the literature review is made.

Chapter 5 describes the conclusions on the conducted measurements, followed by our discussion and recommendations in Chapter 6.

Chapter 7 lists the references cited in this report.



# 2 METHODOLOGY

## 2.1 INTRODUCTION

The following measurements have been conducted in this project:

- Beach pilot measurements (23-08-2018);
- Offshore measurements (04-06-2019);
- Offshore measurements (20-06-2019).

The offshore EMF measurements were conducted on two transects per cable with a specifically developed measurement sledge device (see paragraph 2.4).

On the two offshore measurement days, transects across the following cables have been measured:

- 04-06-2019: PAWP export cables
- 20-06-2019: LUD, PAWP and OWEZ cables.

Additional to the measurement transect above the cables, also a control transect at approx. 200m distance from the cables was made on the second measurement day.

Below a description of weather conditions during measurements, study area and equipment is given. Also, a description of the analyses that have been done is given.

## 2.2 WIND CONDITIONS & PRODUCTION DATA DURING MEASUREMENTS

Table 2.1 Average wind speed (m/s) during the measurements based on data provided by Eneco.

Date	LUD Wind speed [m/s]	PAWP Wind speed [m/s]	OWEZ Wind speed [m/s]
23-08-2019	<i>Not relevant, since no EMF values were recorded.</i>		
04-06-2019	-	7.5	-
20-06-2019	3.7	4.2	-

Significant wave height was approx. 40 cm on 04-06-2019 and approx. 50 cm on 20-06-2019.

Eneco provided more detailed wind and production data of the two offshore measurement days for the LUD and PAWP OWFs for the purpose of analyses (see Figure 2.1). No wind and production data was provided for OWEZ. Note that power production varies with wind speed, however due to confidentiality only averaged wind speeds are shown in this report.





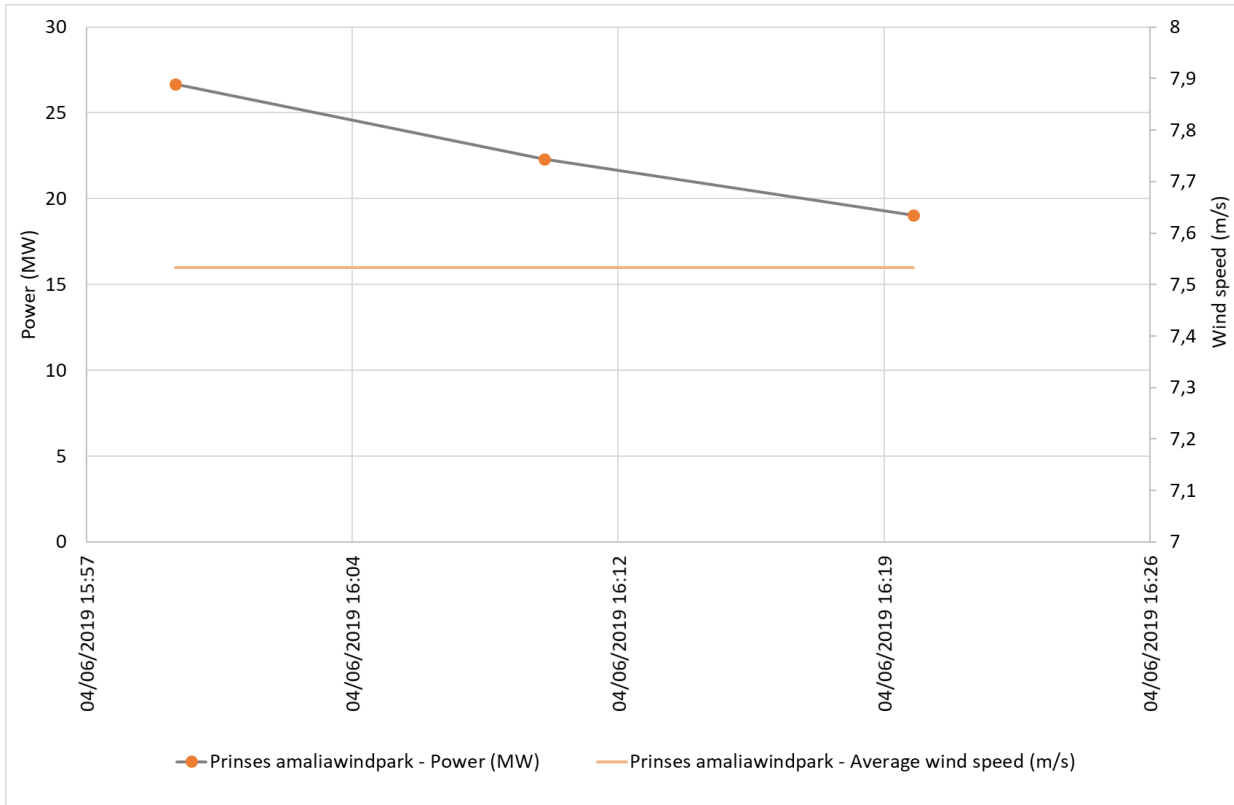


Figure 2.1 Average wind speed (m/s) and production (export power in MW) during EMF measurements on 04-06-2019 (only measured at PAWP).

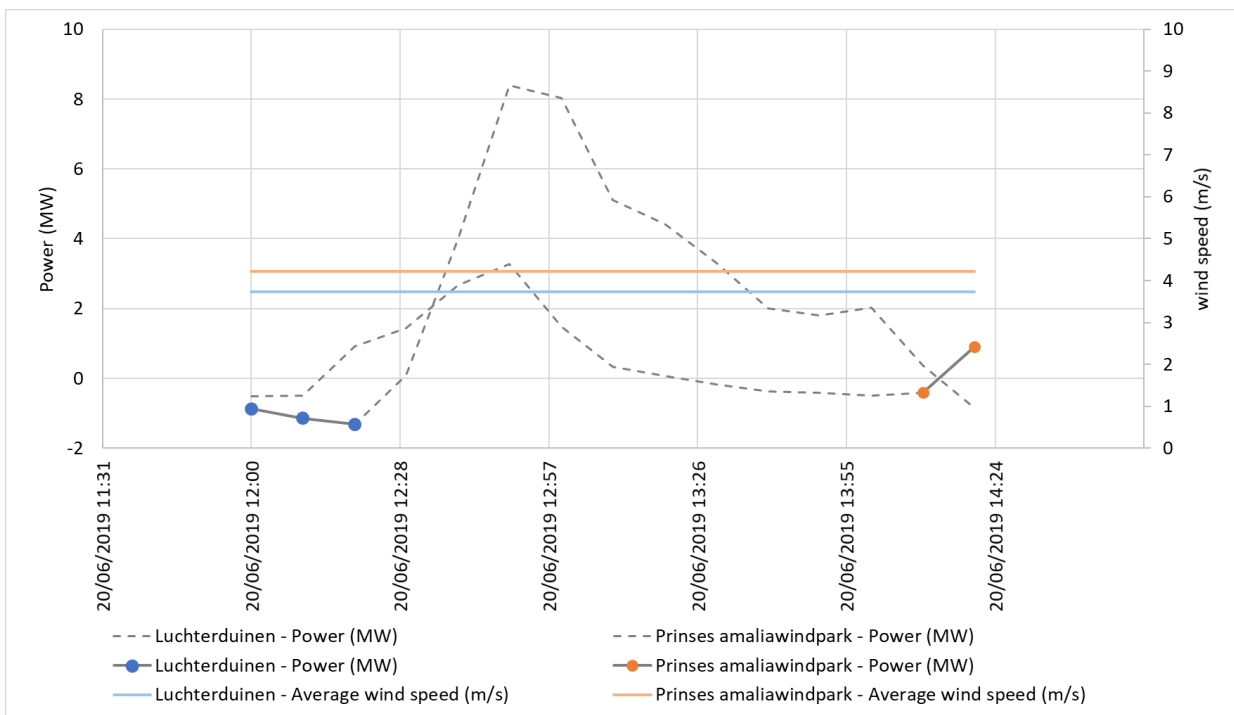


Figure 2.2 Average wind speed (m/s, measured at both OWFs) and production (export power in MW) during EMF measurements on 20-06-2019 (LUD and PAWP, dashed line indicate production, solid line indicate production during EMF measurement timeframe). Note that negative production means that power from shore to OHVS station is transported to keep equipment at the OHVS running.

## 2.3 STUDY AREA

All measurements were done above AC cables (with 50Hz frequency) within the Dutch coastal zone (Table 2.2).

Note that infield cables were not taken into account at this stage due to restricted access in the wind farm areas.

Table 2.2 Overview of three wind parks with corresponding AC undersea export cables, used for this study.

Wind park	Electric power capacity at full production	Voltage
LUD	129 MW	150 kV
PAWP	120 MW	150 kV
OWEZ	108 MW	3 x 34 kV

The study area and location of the measured cables is shown in Figure 2.3.

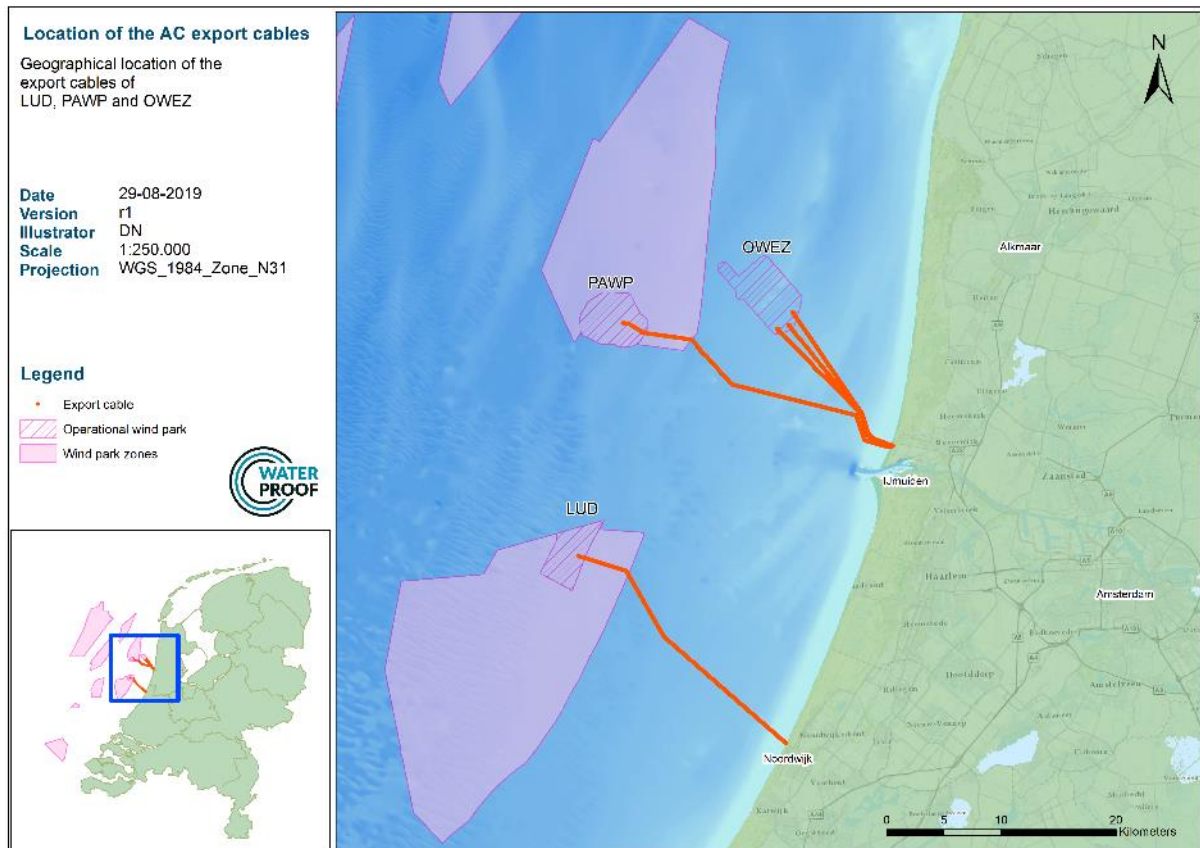


Figure 2.3: Study area and location of the five AC export cables (orange).

### 2.3.1 Cable burial

Cables are generally buried in the sediment to protect the cables (e.g. from anchors, bottom trawling) and to minimize impact on the marine environment. Since EMF strength is strongly related to distance

to the cable, the burial depth of the measured cables is a relevant factor to take into consideration in both planning of the location of the measurements and analyses of the data.

The cable burial for all three wind parks was analysed, based on the most recent bathymetry data. The cable burial history for LUD, PAWP and OWEZ can be seen in Figure 2.4, Figure 2.5 and Figure 2.6 respectively.

The measurement locations were selected based on their burial history with preferences for locations with a constant depth of cable burial and a current burial depth of minimal 1.5 meter to prevent damage to the measurement sledge and cable as requested by the wind farm operators. Table 2.3 presents the corresponding kilometer-points (KP's) of each cable between which the measurements took place. Note that the numbering of the KP's for PAWP and OWEZ starts at the coast ascending towards the wind park, while it is in reverse direction for LUD.

Table 2.3 : Measurement locations (KP's) export cables LUD, PAWP and OWEZ.

Wind park	KP's between which was measured
Luchterduinen*	KP 20 – KP 21
PAWP	KP 8 – KP 10
OWEZ	KP 4 – KP 5

\* KP's calculated from the OHVS

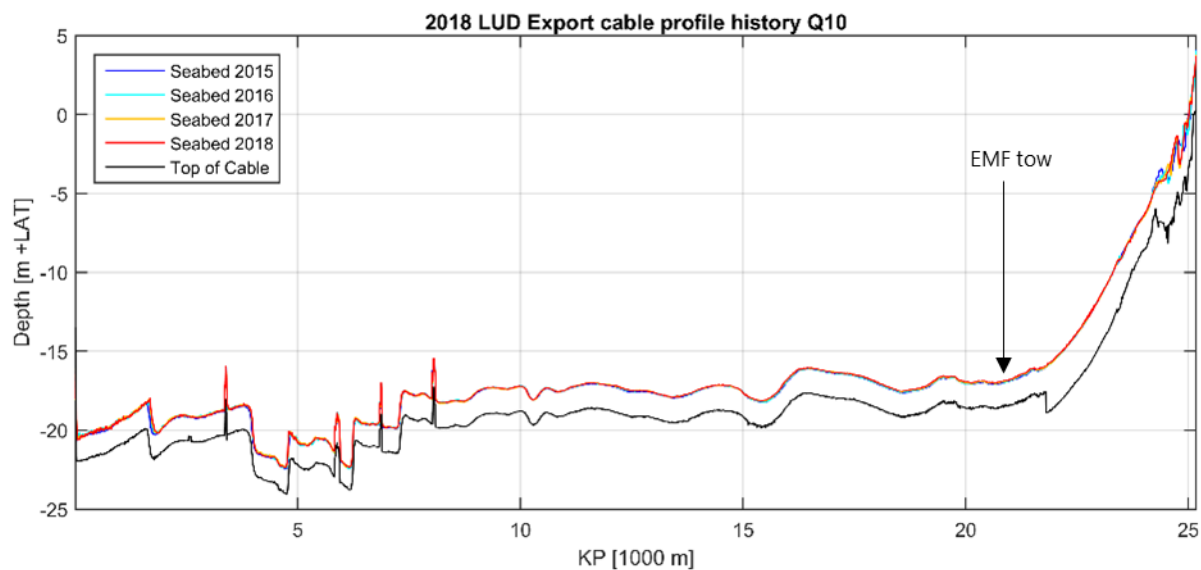


Figure 2.4: Cable burial export cable LUD (data from 2015-2018) with indication (black arrow) of position EMF tow (note that KP0 represents the start of the cable at the offshore OHVS and ~KP25 the shore, as provided by the OWF operator).

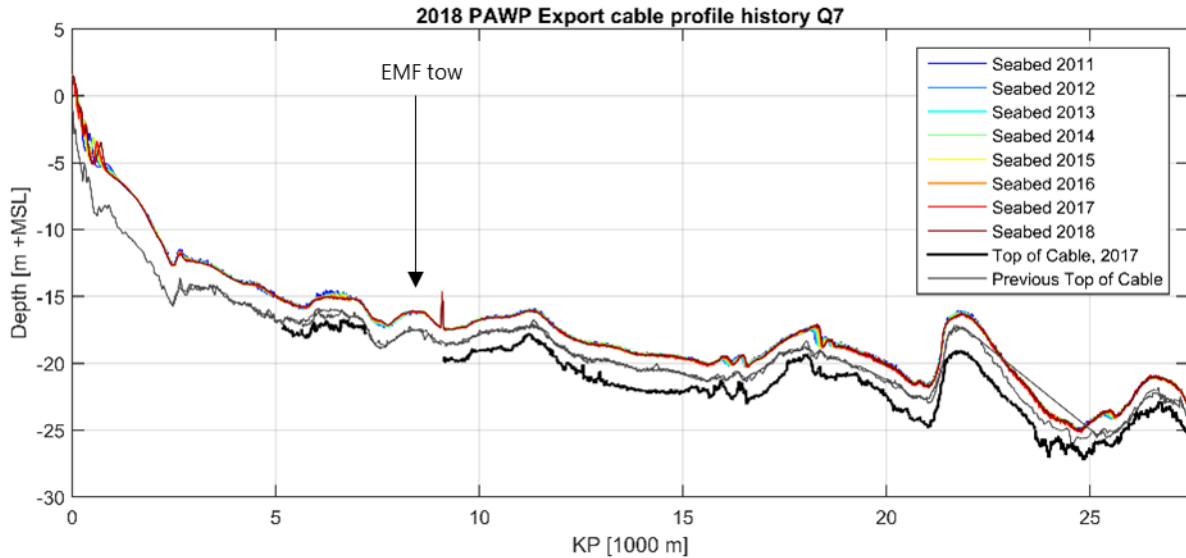


Figure 2.5: Cable burial export cable PAWP (data from 2011-2018) with indication (black arrow) of position EMF tow (note that KP0 represents the start of the cable at the shore and ~KP27 the offshore OHVS, as provided by the OWF operator).

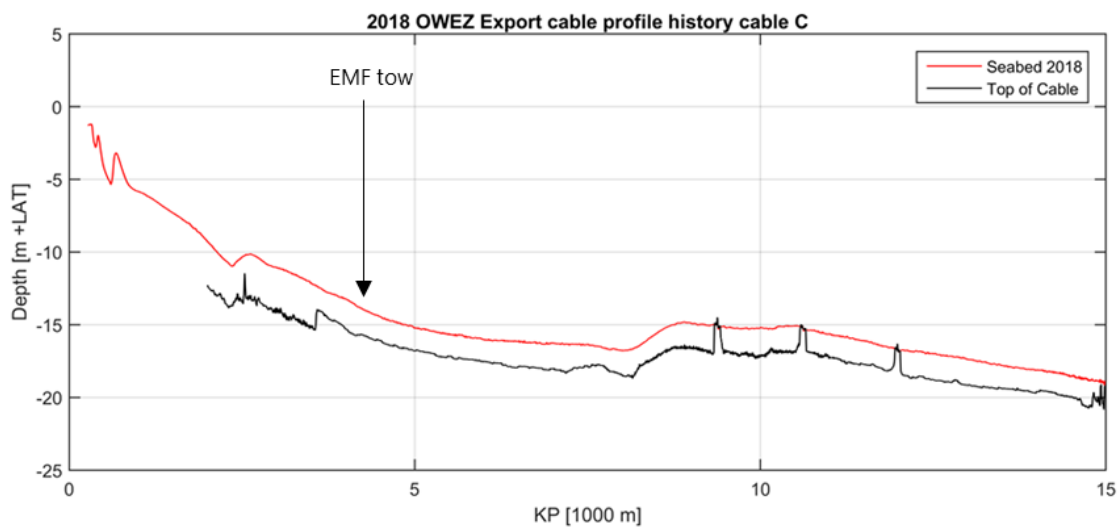


Figure 2.6: Cable burial export cable OWEZ (data from 2015-2018, only cable C is shown) with indication (black arrow) of position EMF tow (note that KP0 represents the start of the cable at the shore and ~KP15 the offshore OHVS, as provided by the OWF operator).

### 2.3.2 Measurement locations

Figure 2.8 shows the location of the offshore measurements, conducted at PAWP on 04-06-2019. The transects are displayed in blue and are labeled "a" and "b", indicating the sequence with "a", being navigated first and "b" second. They were selected around KP 8, due to the (sufficient) cable burial as well as stability of the seabed. The measurement locations of LUD, PAWP and OWEZ during the field campaign on 20-06-2019 are shown in Figure 2.7, Figure 2.9 and Figure 2.10 respectively. All figures show the cable burial as determined in 2018. A more detailed cable burial depth is shown in paragraph 2.3.1.

For all measurement locations, two transects were navigated across the cable of the wind park and across the three cables of the wind park OWEZ. The exact location of each transect and burial depth based on most recent survey data at these transects is presented in Table 2.4.

Note that burial depth of the cables need to be interpreted with caution due to accuracy of (1) initial cable burial depth, (2) annual burial depth surveys and (3) dynamics of the seabed. Small deviations might be present.

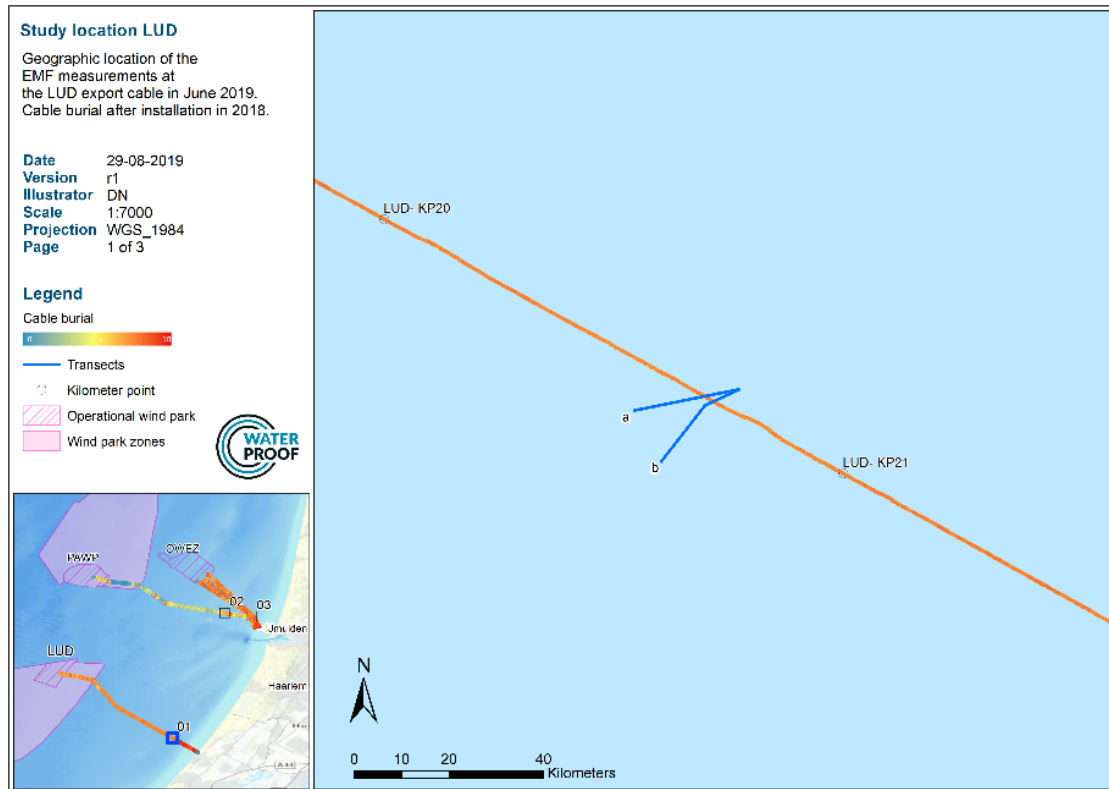


Figure 2.7: Location of the measurements above export cable of LUD (20-06-2019) with cable burial and transects shown in blue indicating the sequence with "a", being navigated first and "b" second.

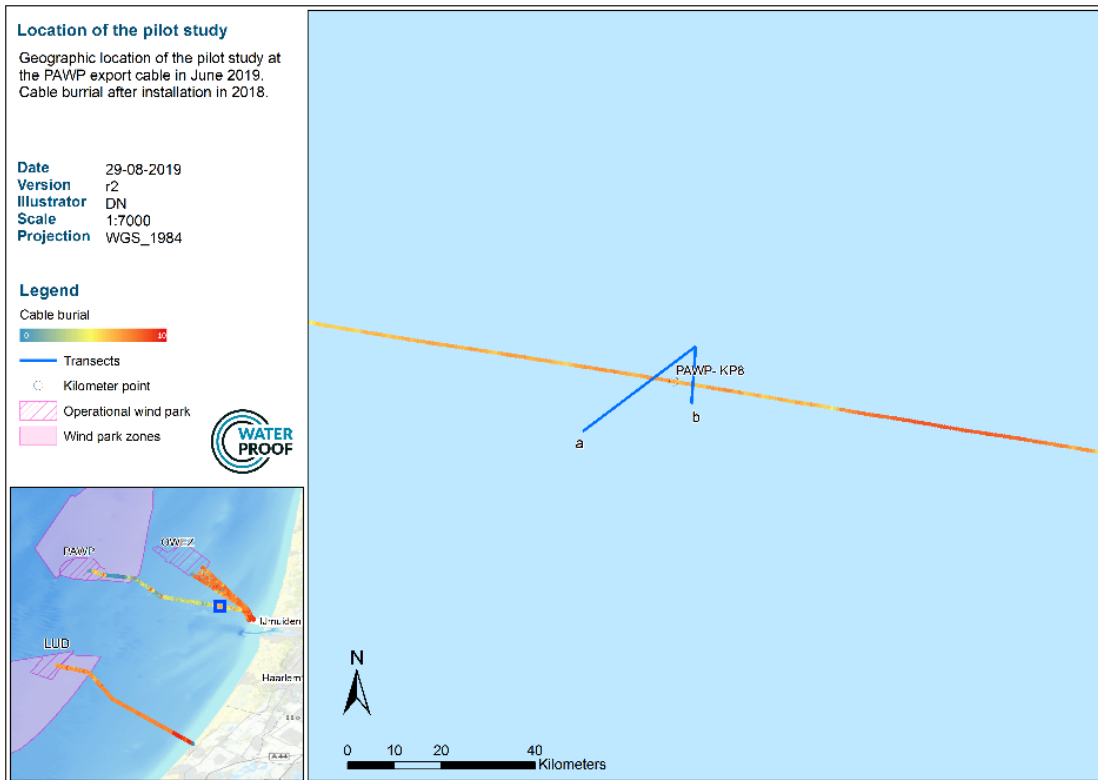


Figure 2.8: Location of the pilot measurements, conducted at PAWP (04-06-2019). Measurement transects are shown in blue indicating the sequence with "a", being navigated first and "b" second.

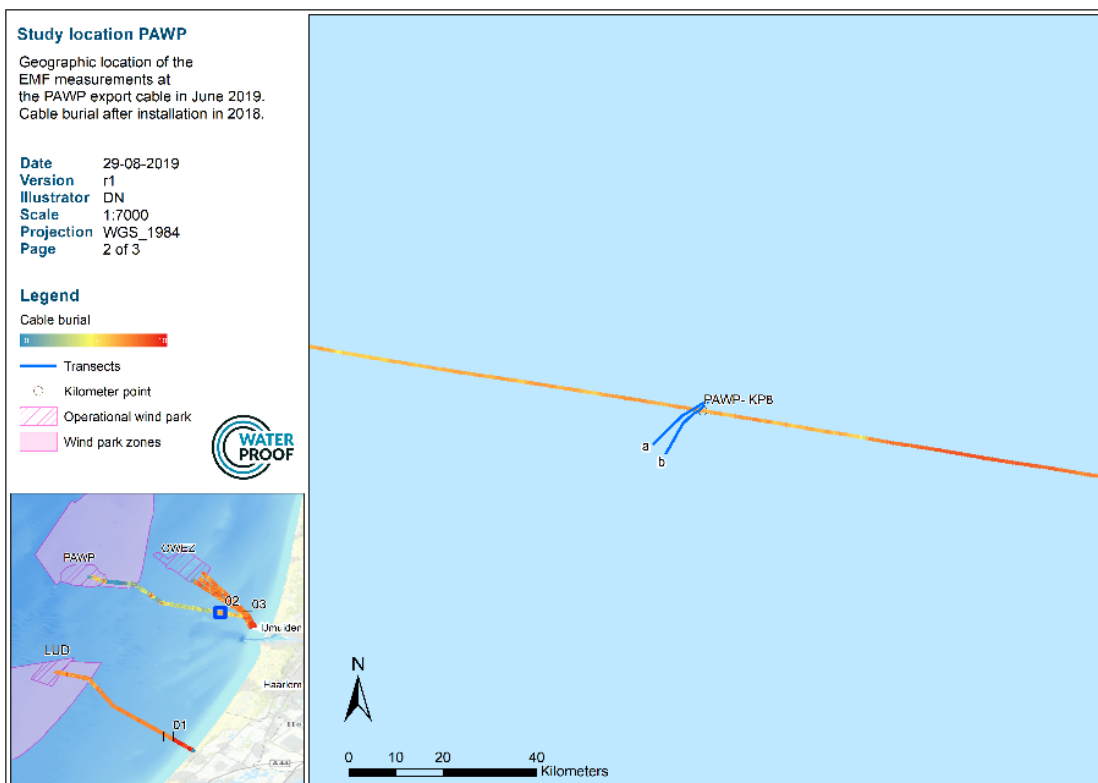


Figure 2.9: Location of the measurements above export cable of PAWP (20-06-2019) with cable burial and transects shown in blue indicating the sequence with "a", being navigated first and "b" second.

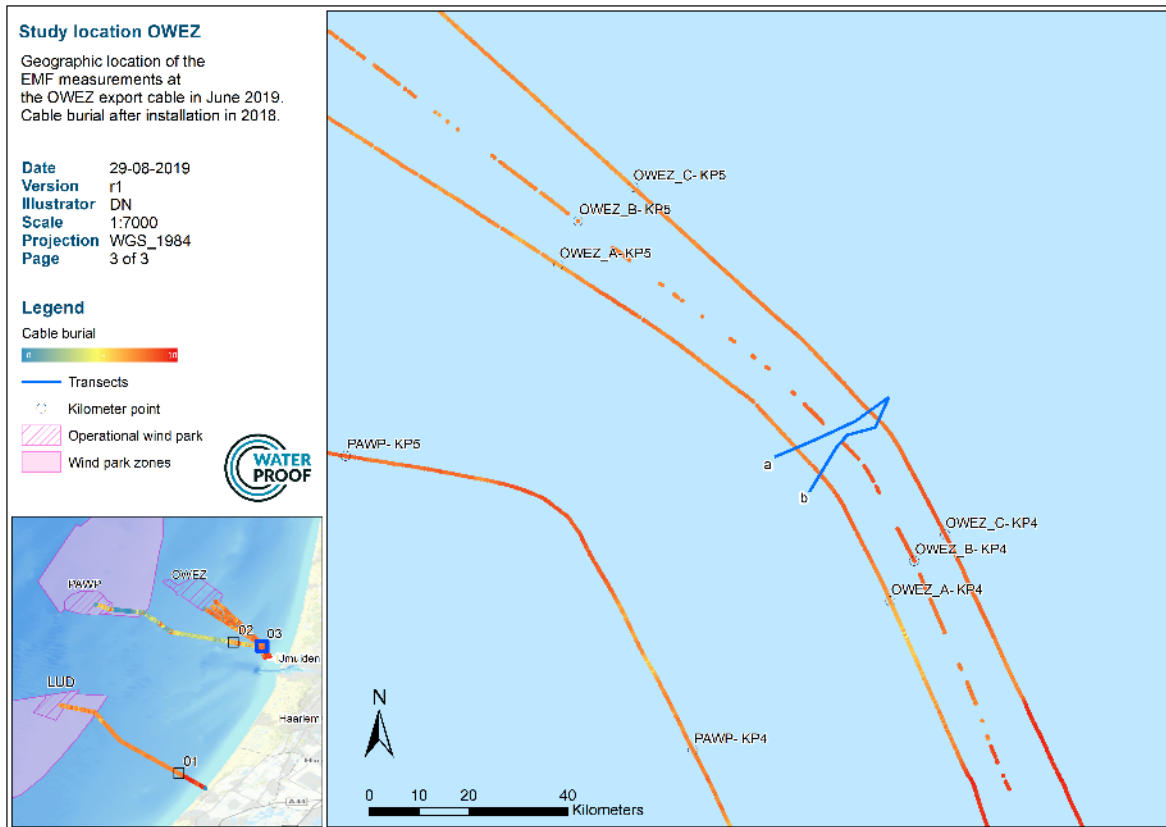


Figure 2.10: Location of the measurements above export cable A, B and C of OWEZ (20-06-2019) with cable burial and transects shown in blue indicating the sequence with "a", being navigated first and "b" second.

Table 2.4 Location of EMF measurements for each cable and each transect in respect to its KP, selected to be in the similar burial depth range (1.5-1.9m).

Cable	Transect (a)		Transect (b)	
	Location above the cable (KP)	Approx. burial depth (m)	Location above the cable (KP)	Approx. burial depth (m)
LUD	KP 20.68	1.6	KP 20.73	1.6
PAWP	KP 8.15	1.5	KP 8.05	1.5
OWEZ A	KP 4.42	1.7	KP 4.34	1.7
OWEZ B	KP 4.35	1.9	KP 4.31	1.9
OWEZ C	KP 4.33	1.8	KP 4.3	1.8

## 2.4 EQUIPMENT

### 2.4.1 Set up

The EMF measurements were done using a measurement sledge that was specifically developed for measuring across the seabed. While navigating each transect at the different locations, the sledge was pulled over the seabed across the undersea export cables.

The sledge has integrated calibrated tri-axial sensors (Narda B-Field probe 100cm<sup>2</sup>) as well as underwater cameras for video observations. All EMF values were logged real-time on board of the survey vessel. Therefore, it was possible to adjust positions and conduct the measurements precisely across and above the undersea export cables.

Combined EMF and video transects were a minimum of ten minutes in duration and estimated to be a minimum of 150 metres long. At each measurement location, the survey vessel was positioned at opposite side of the cable of where the measurement sledge was deployed. Subsequently, the measurement sledge was reeled in hand-controlled (safety measure) and the operator had sight of EMF values (e.g. possible to slow down the movement during fast increase of the EMF values).

Due to the video observations made directly above the export cables, determination of the presence of marine megafauna was possible. The measurement set-up as well as instrument set-up is shown in Figure 2.11.

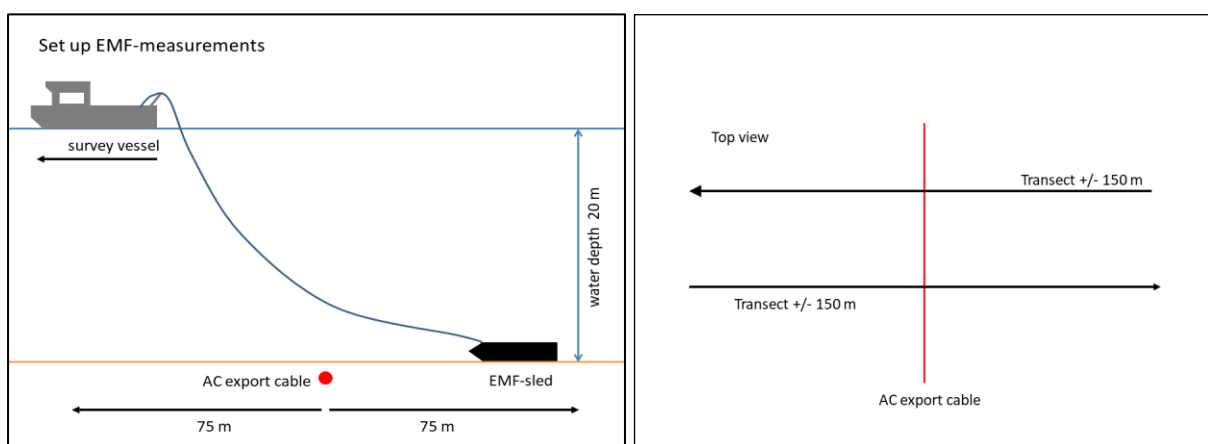


Figure 2.11: Illustration of measurement and instrument set-up. Left: profile and right: top view.

## 2.4.2 EMF-instrument

The measurement sledge to measure EMF at sea was developed by Waterproof. Existing calibrated sensors (Narda ELT-400, Narda B-Field probe 100cm<sup>2</sup>, see Appendix B) were used with bandwidth of frequencies ranging from 30 Hz to 400 kHz and with a resolution of 1 nT. Sensors were connected to a micro-controller and umbilical for transmission of the data to the vessel.

The sensors are mounted in the measurement sledge submersible housing together with autonomous underwater cameras (see below) (Figure 2.12).

An umbilical cable also connects the instrument with a computer on board of the survey vessel allowing real-time data observations on board. Output data in Tesla is logged at a frequency of 4 Hz (4 times per second). Acquisition software for remote control of the sensors was developed and operated from the vessel.

The umbilical cable is labeled every 10 meters in order to determine the distance between vessel and instrument. A surface float equipped with GPS tracker was connected to the measurement sledge, to track the approximate position of the measurement sledge during measurements.

Additionally, by keeping some tension at the umbilical cable, the cable was kept free from the seabed during the execution of the measurements to avoid disturbance of megafauna prior to the actual measurements with the sledge.



The maximum EMF values that can be detected with the set-up of the instrument were limited to 320  $\mu\text{T}$  which was assumed beforehand to be a sufficient range for maximum EMF values. Since the EMF of interest are of high frequencies, the static earth magnetic field of approximately 50  $\mu\text{T}$  (at the study area) did not affect the measurements. However, there is a very small dynamic EMF produced by the earth magnetic field, which is included in our measurements as a background value of approximately 0.0325  $\mu\text{T}$  (See also section 3.2).



*Figure 2.12: Measurement sledge for EMF measurements and video observations (camera system not installed here), with umbilical cable.*

### 2.4.3 Underwater camera system

Towed systems with under water cameras are used for monitoring of mega-epibenthic and macro-epibenthic fauna, including mobile species, for decades (Mallet & Palletier 2014).

The camera system comprises three different Go-Pro video cameras that were attached to the sledge to film the seafloor and assess the benthic landscape and mobile species. The camera objective was situated 5-10 cm above the seabed (there is no contact of the camera with the seabed) with a sideward directed angle of 80°, which is close enough to identify species under varying visibility conditions, while still offering a large enough field of view for habitat description.

Cameras were placed in opposite sides so that images could be retrieved independent of the direction of the EMF sledge on the sea floor. A third camera was used as a spare in case other cameras failed.

One LED light (underwater LED Walkefire) is fixed parallel to the cameras at an suitable angle to cover the entire field of view of the video camera.

Timing was essential in order to synchronised images and EMF values, therefore, apart from the digital time recording of the video recordings, cameras were synchronized with the EMF measurement device (see next paragraph).

## 2.4.4 Synchronizing camera and EMF sensors

The cameras of the measurement sledge were synchronized with the EMF sensors on board of the survey vessel. A synchronization is important to exactly couple video images and species identification to measured EMF values. Once time-synchronized, we have certainty that the video observations are made exactly above the cable, based on the real-time peak detected by the EMF instrument.

The synchronization was done on the first day by generating an EMF on board, recording simultaneously with the cameras and register the exact time. The generated EMF was approximately 0.16  $\mu\text{T}$ . This was repeated three times and strength and moment of the generated EMF can be seen in Figure 2.13. On the second measurement day, time was recorded at the start of each transect and synchronised to EMF measurements.

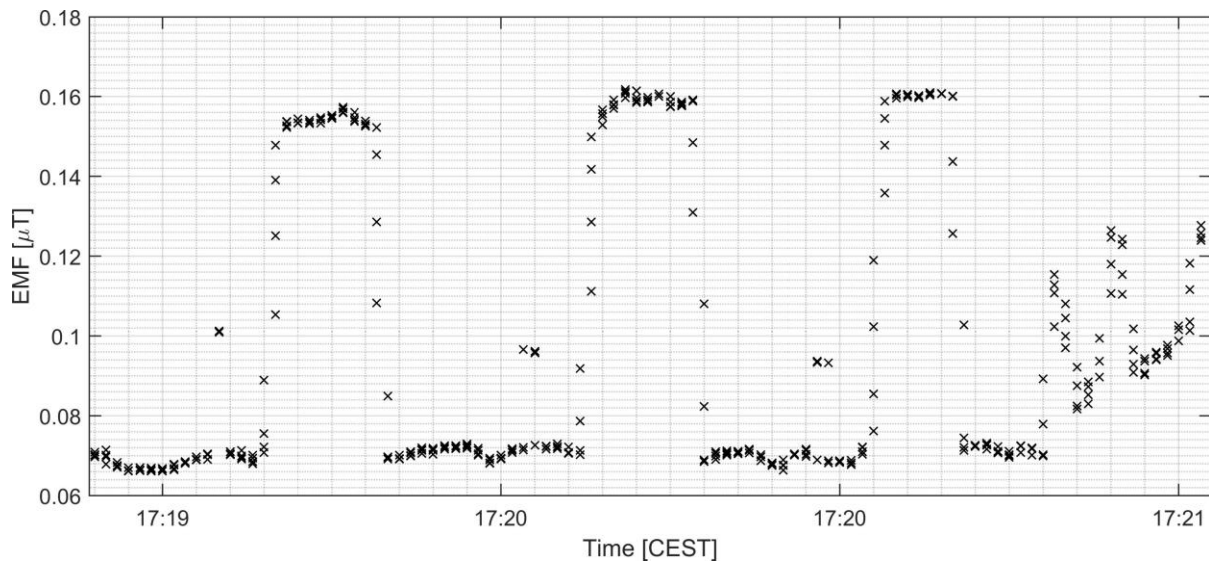


Figure 2.13: Generated EMF fields (three peaks) on board of the vessel in order to synchronize EMF sensors and underwater cameras.

## 2.5 SURVEY VESSEL BUMBLEBEE

All measurements were conducted using the survey vessel *Bumblebee* of Waterproof (Figure 2.14). Disturbances of the EMF measurements are minimized due to the vessel's polyester hull compared to steel hull of larger vessel.



Figure 2.14: Survey vessel Bumblebee of WaterProof BV.

## 2.6 ANALYSIS

### 2.6.1 EMF measurements

The raw EMF data as logged from the EMF-sensors with output frequency of 4 Hz was plotted. Subsequently, it was determined if by means of the real-time output of the measurement sledge the subsea power cables could be detected.

In order to analyze the data, prevailing wind conditions provided by Eneco were used (see Section 2.2)

### 2.6.2 EMF calculations

EMFs are direct proportional to the electric current (ampere). Hence, the larger the electric current, the larger the induced EMF around the cable. To predict EMF around cables, models are generally used.

One of the initial objectives of this study was to validate the EMF models used to predict EMFs. However, due to the use of a small survey vessel to prevent (electrical) disturbance of the measurements, it was in this study only possible to measure under very low wind conditions (2-4 Bft). As a result, production of the measured OWFs was very low during measurements.

Due to this very low production (or even negative in case of power supply from shore to the OHVS stations) it was unfortunately not possible to make a solid comparison of the measured EMF values at this stage to modelled values. EMF calculations are therefore not further included in this report. For further model validations, reference is made to the recommendations in Sector 6.4.

## 2.6.3 Camera footage

### Image selection

First, a selection of camera footage used for analyses was made for each transect. For each transect one camera is filming the sea floor whereas the other consequently is filming the pelagic. The images of the sea floor were selected for further processing, as pelagic footage showed no marine life present.

To create the subsection of images for analysis, 10 seconds of each two minutes was used in every transect and repeated until the transect end time was reached. During the periods that the measurement sledge was approaching the cable (measured by the EMF peak on board of the vessel), a 3 times 10 seconds interval was used (totaling 30 s) for each minute above the cable, in order to also record detailed changes over time until the end of the peak was reached.

The number of images used for analyses for each cable is shown in Table 2.5.

*Table 2.5: Number of images used for analysis*

	Start – End peak transect (a)	Start – End transect (b)	Total number of recordings analysed
Test: PAWP cable	16:03-16:04	16:17-16:20	38
LUD cable	13:05-13:10	13:18-13:22	42
PAWP cable	15:08 -15:14	15:17 -15:20	38
OWEZ cable	16:00-16:03	16:36-16:40	40
	16:12-16:16	16:42-16:44	
	16:24-16:28	16:50-16:52	

### Qualitative description

For each selected image, a brief qualitative description was made of 1) the seabed 2) mobile species present 3) epifauna species present 4) obvious behavior of species 5) quality of the images. Abundant species were quantitatively assessed using a Braun-blanquet classification (see Table 2.6). The seabed was inspected for obvious structures and sediment characteristics. Obvious structures include sand ripples and holes created by benthic infauna. Sediment was, based on image analysis, classified as sand, muddy sediments, gravel or shell fragments. Shell fragments were estimated in percentage to the nearest %.

*Table 2.6: Braun-blanquet scale*

Symbol	Cover	Abundance	Number
r	≤1%	1 specimen	1
+	≤1%	2-5 specimen, sparsely or very sparsely present	2
1	≤5%	6-50 specimen, plentiful	3
2m	≤5%	>50 specimen, plentiful but sparse cover	4
2a	5% - 15%	-	5

2b	16% - 25%	-	6
3	26% - 50%	-	7
4	51% - 75%	-	8
5	76% - 100%	-	9



# 3 RESULTS EMF'S

In this chapter, the results of the EMF measurements are described. The results of the analyses of the video observations by Bureau Waardenburg are described in chapter 4.

## 3.1 BEACH PILOT 2018

In preparation to the offshore field measurements, a beach measurements campaign was conducted by WaterProof and Bureau Waardenburg on 23-08-2018 at the beach and shallow water above the PAWP cable. The aim of these measurements was to test the measurement sledge behavior, and influence of the GoPro cameras on the EMF measurements.

From these beach measurements, the following lessons were learned:

- There was no influence of the GoPro's on the EMF measurements at distances larger than 10 cm from each other. The positioning of the cameras on the sledge have been based on these tests;
- The measurement sledge was stable in behavior in shallow water, though it needs additional weight to keep the sledge at the seafloor while being towed;
- If the sledge lands on it side, it will move by itself to the correct towing position, though there is a chance that the sledge lands upside down. This has no influence on the EMF measurements, though it was decided to position an additional GoPro camera to ensure correct video observations;
- The position of the EMF sensors in the sledge did not influence the EMF field strengths, as there was limited space to move the sensors further away from the seafloor (5-10 cm).
- Measurements in shallow water did not differ from measurements at the beach.
- Measurement settings were optimized based on measurement results.

The actual measurement values (EMF strengths) were not part of the objective of the beach pilot in 2018 and have therefore not been registered.

## 3.2 OFFSHORE EMF FIELD VALUES

During the measurements in 2019, a clear increase in EMF values from background values was observed directly above all cables (LUD, PAWP, OWEZ). Since every cable was crossed twice, two peaks can be associated with one export cable.

### 3.2.1 Luchterduin (LUD)

The export cable of LUD causes the occurrence of two clear EMF peaks (Figure 3.1). Background EMF values of approximately  $0.032 \mu\text{T}$  were measured before and after the cable and are considered as a background (earth-magnetic) EMF value.

Two clear peaks in EMFs are measured while crossing the cable. The first EMF peak had a maximum of  $0.0356 \mu\text{T}$  ( $3.56 \cdot 10^{-8}\text{T}$ ), whereas the second peak had a maximum value of  $0.0363 \mu\text{T}$  ( $3.63 \cdot 10^{-8}\text{T}$ ). Both peaks correspond to the moment of crossing the export cable with the measurement sledge, based on the timing and position of the measurement sledge.

Considering a background value of  $0.032 \mu\text{T}$ , the export cable at LUD causes an elevation of the EMF of  $0.004 \mu\text{T}$ . The EMF strength measured at LUD is smaller compared to the other offshore wind parks, which could be due to lower electric currents, better shielding of the cable or different burial depth.

The control measurements at 200m distance from the cable showed similar background values.

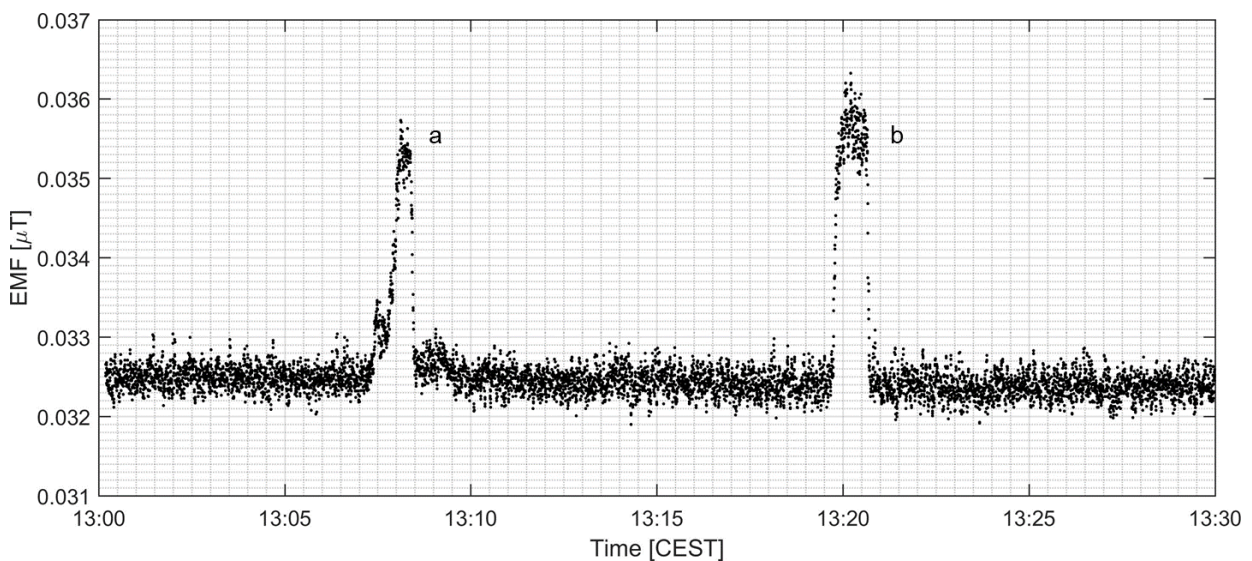


Figure 3.1: Measured EMF above the export cable of OWF Luchterduinen (LUD) on 20-06-2019. Note that the width of the EMF peak is determined by the survey speed.

### 3.2.2 PAWP

Measurements at the export cable of PAWP were conducted twice on two separate measurement days. First measurements were conducted on 04-06-2019, with results shown in Figure 3.2. Two clear increases of the EMF can be observed. The first peak had a maximum of  $0.071 \mu\text{T}$  ( $7.1 \cdot 10^{-8}\text{T}$ ), the second peak shows an increase to  $0.052 \mu\text{T}$  ( $5.2 \cdot 10^{-8}\text{T}$ ). Taking into account a background value of  $0.0325 \mu\text{T}$ , the export cable caused an increase in EMF of  $0.039 \mu\text{T}$  and  $0.02 \mu\text{T}$  for transect (a) and transect (b), respectively.

Although measured across the same export cable, the two peaks vary in value. This might e.g. be due to local variations in cable burial or varying wind speed, though actual differences in measured EMF values are limited.

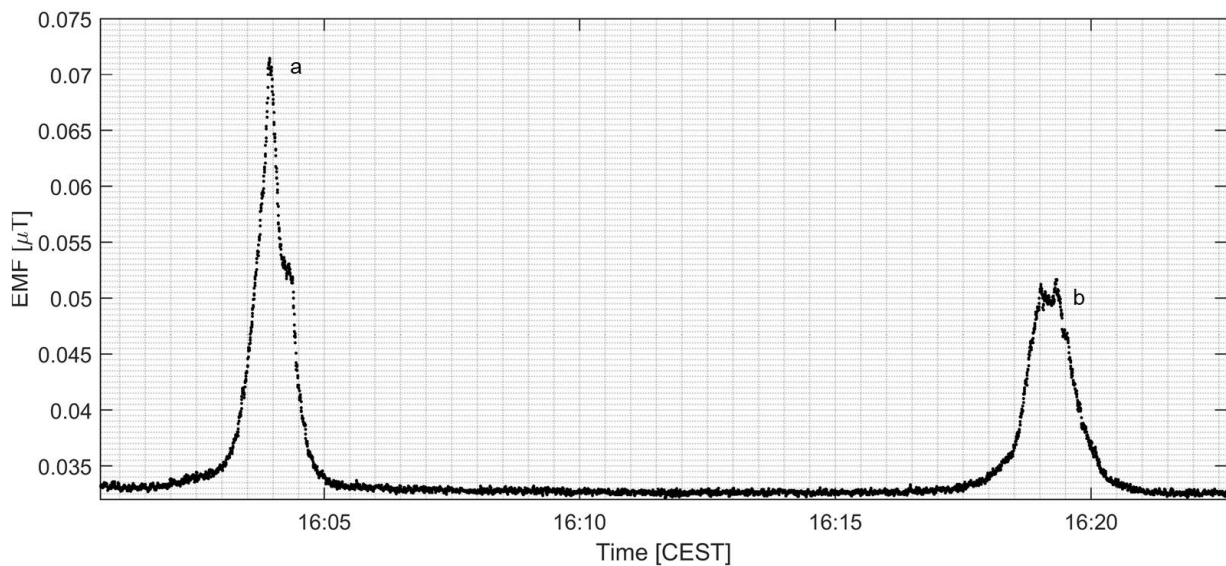


Figure 3.2: Measured EMF above the export cable of the wind park Prinses Amaliawindpark (PAWP) on 04-06-2019. Note that the width of the EMF peak is determined by the survey speed.

Similar to the results of the first day, the second field campaign day at PAWP also revealed clear increase of EMF's above the export cable (Figure 3.3).

The first measured peak reaches a maximum value of 0.049 μT ( $4.94 \cdot 10^{-8}T$ ). The second peak is lower with a maximum value of 0.046 μT ( $4.6 \cdot 10^{-8}T$ ).

These results show that the export cable caused an increase of EMF relative to its surroundings. While the overall background value was found to be 0.0325 μT, the increase of the peaks was approximately 0.015 μT greater than this value.



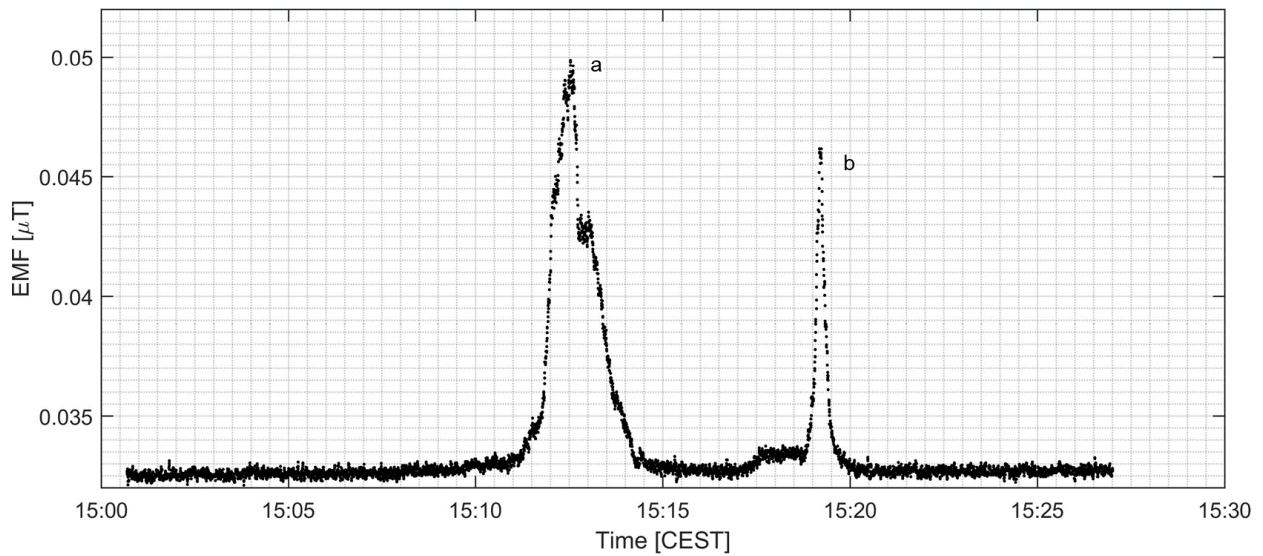


Figure 3.3: Measured EMF above the export cable of OWF Prinses Amaliawindpark (PAWP) on 20-06-2019. Note that the width of the EMF peak is determined by the survey speed.

### 3.2.3 OWEZ

Three export cables connect the wind park OWEZ to shore, hence each measurement transect crossed three cables (Figure 2.10). This can be seen in measured EMF values, showing six peaks in total: Aa, Ab, Ba, Bb, Ca and Cb (see Figure 3.4, cable A, B and C, and crossing the first time (a) and second time (b)).

The measured elevations of EMF above the export cables vary. Peaks reach minimal  $0.04 \mu\text{T}$  ( $4.0 \cdot 10^{-8}\text{T}$ ) for cable A, while cable B shows an increase up to  $0.046 \mu\text{T}$ . Maximum EMF values occur above cable C with  $0.052 \mu\text{T}$  ( $5.15 \cdot 10^{-8}\text{T}$ ).

This means that export cables at OWEZ generate an increased EMF of  $0.008 - 0.02 \mu\text{T}$  relative to the background value of around  $0.0325 \mu\text{T}$ .

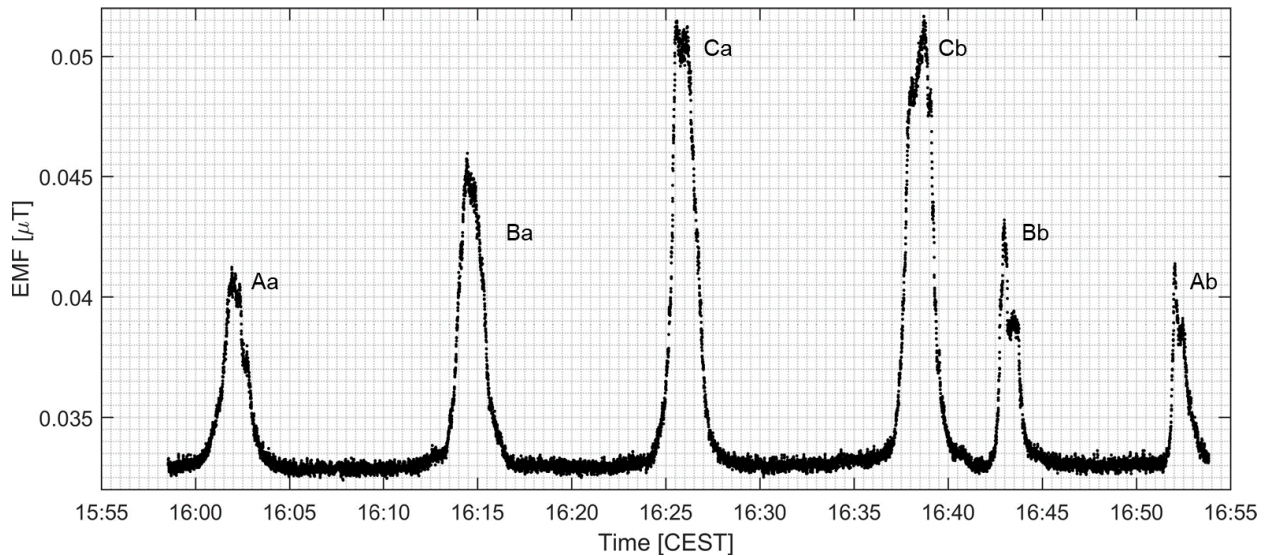


Figure 3.4: Measured EMF above the export cables (A, B, C) of OWF Egmond aan Zee (OWEZ) on 20-06-2019, crossing the first time (a) and second time (b). Note that the width of the EMF peak is determined by the survey speed.

### 3.1 EMF-VALUES VS. POWER

Higher electrical currents generate stronger EMFs. Since the measurements were conducted during low wind speeds and therefore low power production only, the dataset is too limited to make a quantitative assessment of the relation between power and measured EMF values. Nevertheless, Figure 3.5 demonstrates this relation based on the limited data collected.

It is noted that maximum power of LUD, PAWP and OWEZ is 129 MW, 120 MW and 108 MW respectively (see Table 2.2), which is significantly more than the maximum power that is shown in Figure 3.5.

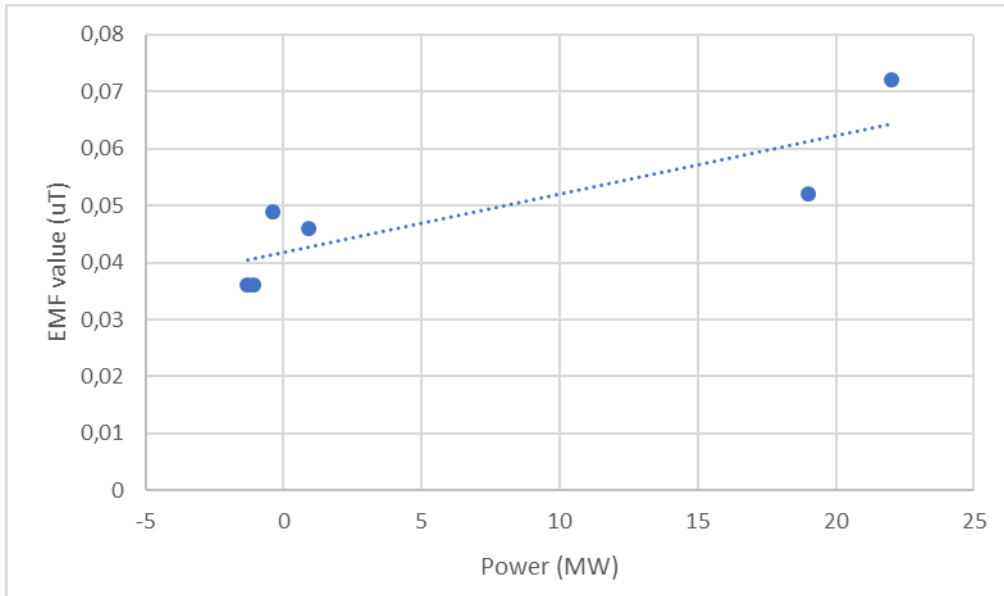


Figure 3.5 Power (MW) vs EMF value (uT), based on the limited measurements conducted above the LUD and PAWP export cables. OWEZ is not included, since no data on power production during the time of measurements was provided.

### 3.2 (POTENTIAL) IMPACT ZONE

Based on the GPS-log of the measurement sledge, the horizontal distances at which increased EMF values on comparison to the background values are determined for all cables measured on 20-06-2020 (shown in Table 3.1). These horizontal distances from the cable give an indication of the potential impact zone around the cables where – under the measured wind conditions and power production - increased EMF values are present.

Table 3.1 Horizontal distance from cable over the seabed at which increased EMF values are measured (in meters at both sides of the cable).

Transect	LUD	PAWP	OWEZ-A	OWEZ-B	OWEZ-C
a	7.5	24.5	14	16.5	23.5
b	7.5	12	18.5	14	23.5

It should be realized that these distances were determined during very low wind conditions. As shown in Figure 3.6, larger distances are expected during higher production.

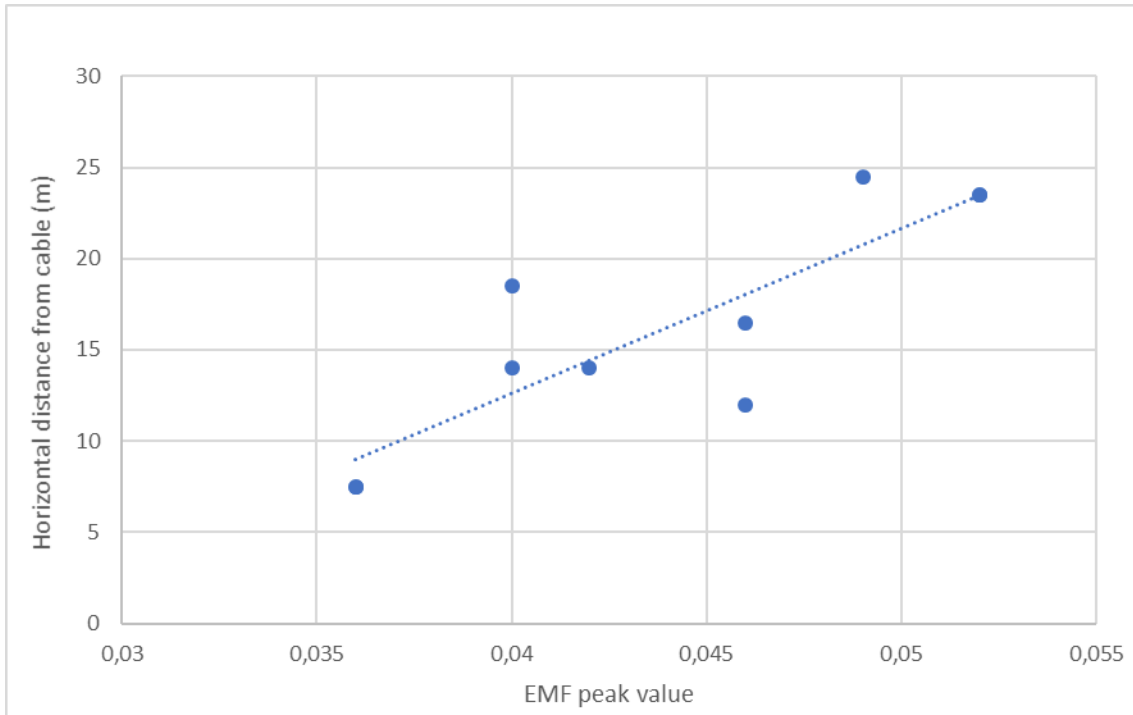


Figure 3.6 EMF peak values directly above the cable vs. horizontal distance from the cable at which increased values in comparison with background values are measured.

# 4 RESULTS MARINE LIFE

In this chapter, the potential impact of EMFs on marine life is determined by means of a field pilot (Section 4.1) and a literature review (Section 4.2).

## 4.1 FIELD PILOT

### 4.1.1 PAWP cable (04-06-2019)

Based on video images analysis, the seafloor around the cable consisted of sandy material with few small ripples and a constant percentage of dead shell material of around 5 %. Depending on the location, filmed topology of the seabed was largely explained by holes and ripples of sea potatoes or sand mason worms.

During the first day, the species (groups) observed around the cable included sea potatoes (*Echinocardium cordatum*), brittle stars (Ophiuroidea), hermit crabs (*Pagurus bernardus* with *Hydractinia echinata*), netted dog whelks (*Tritia reticulata*), gobies (Gobiidae), sand mason worms (*Lanice conchilega*), crabs (*Liocarcinus sp.*) and flatfish (Pleuronectidae) (Table 4.1).

Large aggregations of sea potato moving at the surface were observed in the first part of transect A (Figure 2.8), but not in other areas. Aggregations of sand mason worms were observed in some spots, as were large quantities of brittle stars. Sea potato, sand mason worm and brittle star abundance was varying over the transect and these abundances were used for further analysis. All other species were observed sparsely and with single specimens per image. Therefore, they were not included for further analysis (§2.6).

Interesting behavior include few species being very active, including sea potatoes, brittle stars but also crabs and flatfish. A sea potato was observed to bury itself in the sediment within 60 seconds of images right in front of the camera at the start of transect a.

Although currents were quite strong, images were good enough to estimate species (group) abundance in 90% of the images. Movement of the sledge caused turbidity and yielded some images that were too turbid for interpretation (Table 4.1).



Figure 4.1: Brittle star (Ophiuroidea) and sea potato (Echinocardium cordatum) and a flatfish near PAWP cable (Transect a).

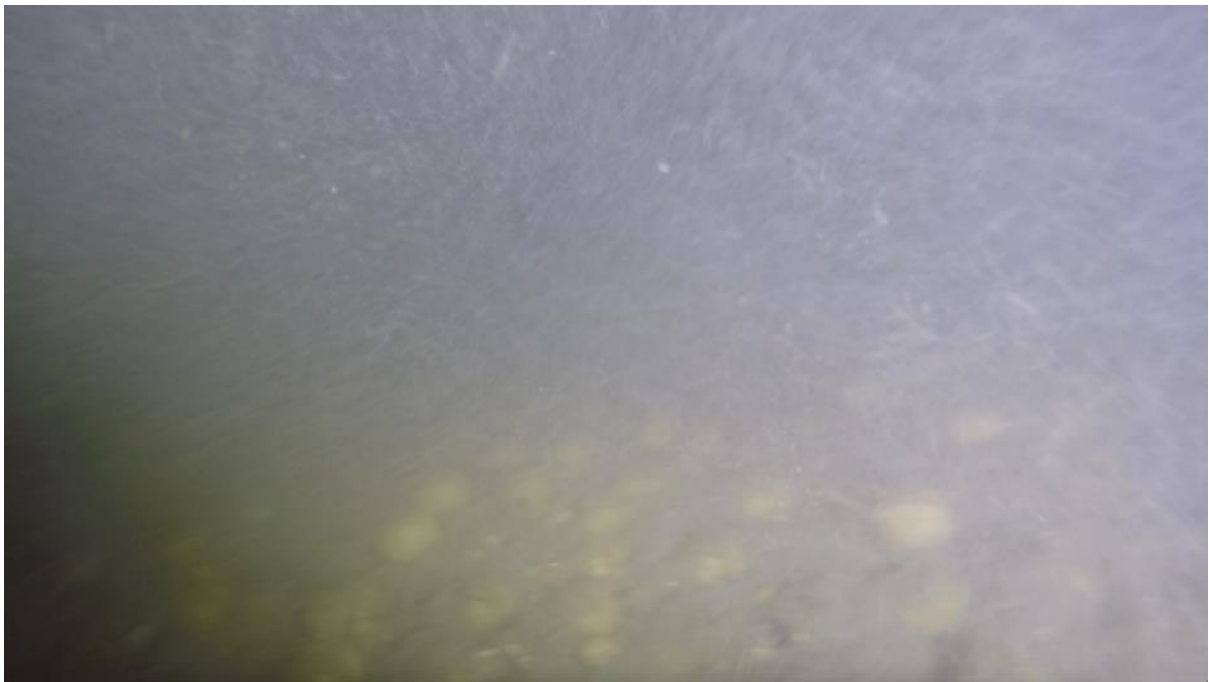


Figure 4.2: Turbid image during movement. Sea potato aggregations are visible but not in detail.

Table 4.1: Qualitative description of species during measurements of transects around PAWP cable, the blue colour indicates the EMF peak.

Time	Description
15:53:00	brittle star sparsely, sea potato plentiful and uncovered (above the sand)
15:54:00	brittle star sparsely, sea potato plentiful and uncovered (above the sand), sand mason worm (sea potato dug into sediment within 60 seconds)

15:55:00	brittle star sparsely, sea potato plentiful and uncovered (above the sand), flatfish (European flounder most likely)
15:56:00	brittle star sparsely, sea potato plentiful and uncovered (above the sand), hermit crab, <i>Hydractinia echinata</i>
15:57:00	no interpretation bad visibility
15:58:00	brittle stars plentiful, sand mason worm
15:59:00	brittle stars plentiful
16:00:00	brittle stars plentiful, netted dog whelk rising from the sea floor, flatfish (European flounder), <i>Liocarcinus</i> , structure resembling eggs
16:01:00	brittle stars on sand, no sea potato, netted dog whelk
16:02:00	brittle stars, no sea potato, shell material abundant
16:03:00	brittle stars, no sea potato, shell material abundant
16:04:00	brittle star sparsely, sea potato sparsely, goby
16:05:00	brittle star sparsely, sea potato sparsely
16:06:00	brittle star sparsely, sea potato sparsely
16:07:00	many brittle stars, one sea potato
16:08:00	brittle star sparsely, sea potato sparsely
16:09:00	no interpretation bad visibility
16:10:00	brittle star sparsely, sea potato sparsely
16:11:00	brittle star sparsely, no sea potato, hermit crab
16:12:00	brittle star sparsely, no sea potato
16:13:00	no interpretation bad visibility
16:14:00	brittle star sparsely, no sea potato, hermit crab
16:15:00	no interpretation bad visibility
16:16:00	brittle star sparsely, no sea potato, hermit crab
16:17:00	no interpretation bad visibility
16:18:00	no brittle stars, one sea potato
16:19:00	brittle star sparsely, no sea potato
16:20:00	no brittle stars no sea potato, netted dog whelk
16:21:00	no interpretation bad visibility

#### 4.1.2 LUD cable (20-06-2019)

Based on video images analysis, the seafloor around the cable consisted of mostly sandy material with few small ripples, half of the transect area also had a small percentage of dead shell material of around 1 %. There were few indications of benthic fauna in the sand (i.e. holes) and epifauna (e.g. the sand mason worm) was only sparsely present. In one image the presence of a lugworm was filmed.

Species groups observed around the LUD cable included common dragonet (*Callionymus lyra*), brittle stars (Ophiuroidea), common starfish (*Asterias rubens*), hermit crabs (*Pagurus bernardus* with *Hydractinia echinata*), sand mason worms (*Lanice conchilega*), brown shrimps (*Crangon crangon*), Sagartia anemone (*Sagartia* sp.) (Figure 4.3; Table 4.2).

Very low abundance of both mobile fauna and epifauna was observed and only a single fish species was present in the transects. All species were observed sparsely and at most times with a single specimen per image and could therefore not be included in further analysis (§2.6).

Although currents were quite strong, images were good enough to estimate species (group) abundance in 70% of the cases. Movement of the sledge caused turbidity and yielded some images that were too turbid for interpretation (Table 4.2).



Figure 4.3: Brittle star (*Ophiuroidea*), hermit crab (*Pagurus bernhardus*) and sand mason worm (*Lanice conchilega*) near LUD cable (Transect A).

Table 4.2: Qualitative description of species during measurements of transects around LUD cable, the blue colour indicates the EMF peak.

Time	Description
13:01:11	Sand, sand mason worm sparsely, 1 starfish
13:03:11	Sand, 1 sand mason worm, brown shrimp sparsely, 1 brittle star
13:05:11	Sand, sand mason worm sparsely
13:06:11	Sand and dead shell material, sand mason worm sparsely, brown shrimp sparsely, 1 brittle star
13:07:11	Sand and dead shell material, sand mason worm sparsely, brown shrimp sparsely, 1 brittle star, lugworm piles
13:08:11	Sand and dead shell material, sand mason worm sparsely, 1 brittle star
13:09:11	Sand and dead shell material, sand mason worm sparsely, hermit crab and brittle star sparsely
13:10:11	No interpretation bad visibility
13:12:11	Sand and dead shell material, 1 sand mason worm
13:14:11	Sand and dead shell material, sand mason worm sparsely, hermit crab brittle star sparsely, <i>Sagartia</i> anemone



13:16:11	No interpretation bad visibility
13:18:11	Sand and dead shell material, brittle stars sparsely
13:19:11	No interpretation bad visibility
13:20:11	Sand, common dragonet, brittle stars sparsely
13:21:11	Sand and dead shell material, brittle stars sparsely
13:22:11	No interpretation bad visibility
13:24:11	No interpretation bad visibility
13:26:11	No interpretation bad visibility
13:28:11	No interpretation bad visibility

#### 4.1.3 PAWP cable (20-06-2019)

Based on video images analysis, the seafloor around the cable consisted of mostly sandy material with few small ripples, half of the transect area also had a small percentage of dead shell material of around 5%. There were abundant indications of benthic fauna in the sand (i.e. holes, filtering parts of mollusks, sea potato hummocks), whereas epifauna (e.g. sand mason worm) was present sparsely and only in sparse aggregations in a few images.

Species groups observed around the PAWP cable included sea potatoes (*Echinocardium cordatum*), brittle stars (Ophiuroidea), hermit crabs (*Pagurus bernardus* with *Hydractinia echinata*), netted dog whelk (*Tritia reticulata*) and sand mason worms (*Lanice conchilega*) (Figure 4.4).

Very low abundance of both mobile fauna and epifauna was observed and no fish species was present in the transects. All species were observed sparsely and at most times with a single specimen per image, consequently they could not be included in further analysis (§2.6).

Although currents were quite strong, images were good enough to estimate species (group) abundance in 70% of the cases. Movement of the sledge caused turbidity and yielded some images that were too turbid for interpretation (Table 4.3).



Figure 4.4: Brittle star (*Ophiuroidea*) and infauna holes and hummocks near PAWP cable (Transect a).

Table 4.3: Qualitative description of species during measurements of transects around PAWP cable, the blue colour indicates the EMF peak.

Time	Description
15:01:41	Sand, netted dog whelks and brittle stars sparsely
15:03:41	Sand, brittle stars sparsely, 1 netted dog whelk, 2 hermit crabs
15:05:41	Sand, brittle stars sparsely, netted dog whelks sparsely, 2 hermit crabs
15:08:41	No interpretation bad visibility
15:09:41	Sand and dead shell material, netted dog whelks and brittle stars sparsely, 1 sea potato uncovered
15:10:41	Sand and dead shell material, brittle stars sparsely
15:11:41	Sand and dead shell material, brittle stars sparsely
15:12:31	No interpretation bad visibility
15:12:41	Sand and dead shell material, brittle stars sparsely
15:13:41	Sand and dead shell material, brittle stars sparsely
15:14:41	Sand and dead shell material, brittle stars sparsely, netted dog whelks sparsely
15:16:41	Sand and dead shell material, sand mason worm and brittle stars sparsely
15:17:41	Sand and dead shell material, brittle stars sparsely
15:18:41	No interpretation bad visibility
15:19:11	No interpretation bad visibility
15:19:41	Sand and dead shell material, 1 brittle star, 2 sea potatoes
15:20:41	No interpretation bad visibility

15:22:41	Sand and dead shell material, 1 netted dog whelk, 1 brittle star
15:24:41	No video
15:26:41	No video
15:28:41	No video

#### 4.1.4 OWEZ cable (20-06-2019)

Based on video images analysis, the seafloor around the cable consisted of hard sandy material with few small ripples and almost no dead shell material. There were few indications of benthic fauna in the sand (i.e. holes).

During the testrun, species groups observed around the cable included brittle stars (Ophiuroidea), hermit crabs (*Pagurus bernardus* with *Hydractinia echinata* and *Diogenes pugilator*), brown shrimps (*Crangon crangon*), sand mason worms (*Lanice conchilega*), crabs (*Liocarcinus* sp.) and an unidentified snail (Gastropoda spp.) (Figure 4.5, Table 4.4).

Very low abundance of both mobile fauna and epifauna was observed and no fish were present in the transects. All species were observed sparsely and at most times with single specimen per image and could therefore not be included in further analysis (§2.6).

Although currents were quite strong, images were good enough to estimate species (group) abundance in 90% of the images. Movement of the sledge caused turbidity and yielded some images that were too turbid for interpretation (Table 4.4).



Figure 4.5: Sandy seafloor with brittle star (Ophiuroidea), sand mason worm (*Lanice conchilega*) and hermit crab (*Pagurus bernardus*) near OWEZ cable.



Figure 4.6: Track on seafloor.

Table 4.4: Qualitative description of species during measurements of transects around OWEZ cable.

Time	Description
15:58:33	Sand, 1 sand mason worm
16:00:33	Sand, brittle stars sparsely
16:01:33	Sand, brittle stars sparsely, 1 Gastropoda
16:02:33	Sand, brittle stars sparsely, 1 Gastropoda
16:03:33	Sand, 1 brittle star, 1 small hermit crab
16:05:33	Sand, 1 brittle star, 1 small hermit crab
16:07:33	Sand, brittle stars sparsely. Track (human-induced) seems to be visible.
16:09:33	Sand, brittle stars sparsely, hermit crab sparsely, 2 sand mason worm, 1 crab <i>Liocarcinus</i>
16:11:33	Sand, brittle stars sparsely
16:12:33	Sand, 1 brittle star, 1 hermit crab
16:13:33	Sand, brittle stars sparsely, hermit crab sparsely, 2 sand mason worms, 1 crab <i>Liocarcinus</i>
16:14:33	Sand, 2 fighting hermit crabs, brittle stars sparsely
16:15:33	Sand, <i>Liocarcinus</i> sp., hermit crab sparsely, brittle stars sparsely
16:17:33	Sand, 1 brittle star, 1 hermit crab
16:19:33	Sand, sparsely sand mason worms, brittle stars sparsely
16:21:33	Sand, brittle stars sparsely, hermit crabs sparsely
16:23:33	Sand, brittle stars sparsely, hermit crabs sparsely
16:24:33	Sand, brittle stars sparsely, hermit crabs sparsely
16:25:33	Sand, brittle stars sparsely
16:26:33	Sand, brittle stars sparsely, hermit crabs sparsely, 2 sand mason worms
16:28:33	Sand, brittle stars sparsely, hermit crabs sparsely
16:30:33	Sand, brittle stars sparsely, hermit crabs sparsely

16:32:33	No interpretation bad visibility
16:34:33	Sand, brittle stars sparsely, hermit crabs sparsely
16:36:33	Sand, 1 hermit crab, 1 brown shrimp
16:37:33	Sand, brittle stars sparsely
16:38:33	Sand, brittle stars sparsely, hermit crabs sparsely
16:39:33	Sand, 1 brittle star, 1 hermit crab
16:41:33	Sand, 1 brittle star, hermit crabs sparsely
16:42:33	Sand, brittle stars sparsely, hermit crabs sparsely
16:43:33	Sand, hermit crabs sparsely
16:44:33	Sand, brittle stars sparsely, hermit crab
16:46:33	No interpretation bad visibility
16:48:33	Sand, brittle stars sparsely, hermit crab sparsely
16:50:33	Sand, 1 brittle star, 1 hermit crab, 1 crab <i>Liocarcinus</i>
16:51:33	Sand, 1 brittle star, 1 hermit crab, 1 crab <i>Liocarcinus</i>
16:52:33	No interpretation bad visibility
16:53:33	Sand, brittle stars sparsely
16:55:33	Sand, hermit crabs sparsely
16:57:33	Sand, brittle stars sparsely



#### 4.1.5 Biodiversity in relation to EMF strength

On the first day of field measurements, a piece of seabed was encountered with a rich benthic bottom life consisting of, among other things, a high density of sea potatoes, brittle stars, sand mason worms and flat fish. On the second day of field measurements, this pattern was not observed again. On this second day, species were observed sparsely and at most times with single specimen per image and could therefore not be included in further analysis. Therefore, only images of the PAWP cable at 04-06-2019 were used for further processing.

The quantity of sea potatoes, brittle stars and sand mason worms varied over the transect around the (Figure 4.7). High abundances of brittle stars and sand mason worms were only observed away from the cable (i.e. the area with low EMF strength). Sea potato aggregations with high densities were observed only in areas of low EMF strength, however this pattern was observed only at the start of the transect (Figure 4.7) and not in all other areas with low EMF strength.

Considering that this is only a single observation and no repeated quantitatively research and analysis was conducted, it is merely anecdotal and no firm conclusions could be drawn from the results of this field study.

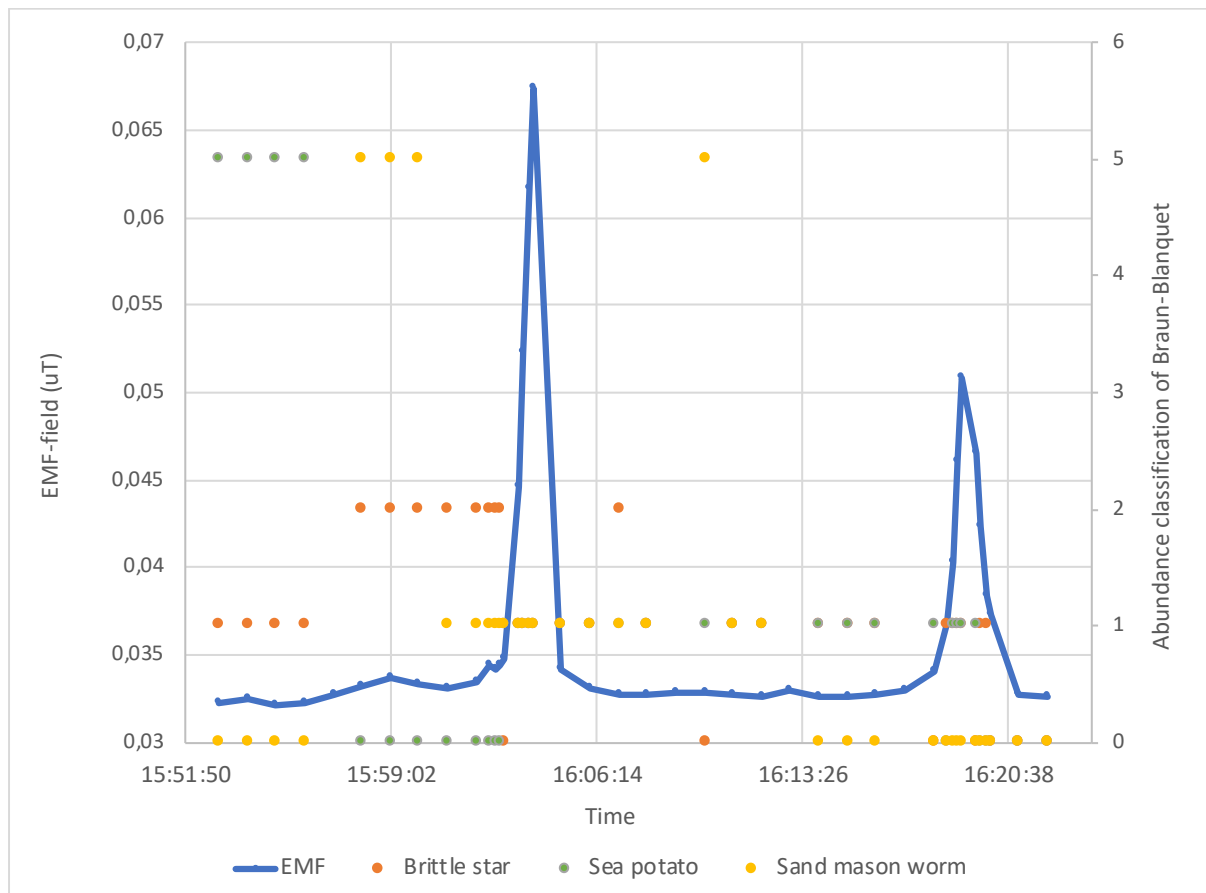


Figure 4.7: Brittle star (*Ophiuroidea*), sea potato (*Echinocardium cordatum*) and sand mason worm (*Lanice conchilega*) abundance in relation to EMF strengths around the PAWP cable at 04-06-2019. Abundance is quantified with Braun-Blanquet classification.

## 4.2 LITERATURE REVIEW

The impact of electromagnetic fields on the marine ecosystem is largely unknown. Limited available literature indicates possible disturbance or avoidance at the cables by certain species. Moreover, data about the impact of EMF induced by cables on species that are specifically present in the Dutch North Sea are lacking. To get more insight in the potential impact of EMFs on species present in the Dutch North Sea, a desk study, which was phase 1 of this project, was carried out. In this paragraph we summarize the main results and add relevant new literature of the years 2017-2019.

### 4.2.1 Desk study on the potential impacts of EMFs on marine ecosystems

Since electric fields are inhibited by shielding material, the obvious effects of subsea cables on biota are generated by either magnetic fields or induced electric fields (iEFs). Movement of organisms through a magnetic field creates induced electric fields, with organisms moving parallel to the cable yielding no induced electric field and organism moving perpendicular to the cable magnetic field generating the maximum induced electric field. These induced electric fields are however not measurable in the field.

In the conducted desk study (Snoek et al, 2016), it was concluded that several taxonomic groups inhabiting European seas are sensitive to EMFs. It is suggested in literature that all species groups sense magnetic fields, whilst electric fields are sensed by invertebrates, bony fish, elasmobranchs and a single dolphin species (Table 4.5). Magnetic and electric fields are used by marine organisms for various ecological functions, like orientation, reproduction, migratory behavior and predator-prey detection.

In the North Sea several subsea power cables are present, and since for instance new wind farms are being constructed, more subsea power cable are planned. The EMFs and iEFs generated by these cables most certainly are in the range that potentially has an effect on the marine environment. Furthermore, lower EMF strengths are not necessarily associated with less impact. Weak EMFs can have an important ecological function, such as the little variations in the geomagnetic field used for navigation during migration and the weak fields induced by prey.

The limited literature suggests that species on each level of the North Sea food web are potentially sensitive to EMFs. High sensitivity is expected for elasmobranchs (sharks, rays), but also invertebrates (crustaceans, molluscs), bony fish and marine mammals inhabiting the North Sea can potentially be affected by EMFs. Benthic species, located closer to cables encounter stronger EMFs and hence are more likely to be affected.

*Table 4.5: Sensitivity of marine species groups to EMF fields (from: Phase 1 report).*

Species (groups)	Sensitivity: Magnetic fields	Sensitivity: Electric fields
Invertebrates	Anecdotal evidence of arthropods and Mollusca's using magnetic field for orientation (e.g. nudibranch, amphipods, isopods and lobsters).  Interference with embryonic and cellular development (e.g. sea urchins), cellular damage in larvae (barnacles).	Anecdotal evidence of electroreception used for prey detection (e.g. crayfish).
Bony fish	Used for daily navigation, long distance migration, homing. Magnetite present in several species including salmonids. Strong evidence is lacking.	Several species use electric sense for prey detection. Ampullae of Lorenzini found in sturgeons and catfishes.
Elasmobranchs	Responses to magnetic field changes described. No explicit proof.	Ampullae of Lorenzini found in elasmobranchs. Used for predator/ prey detection, orientation, and navigation.

Turtles	Earth's magnetic field used for orientation and finding breeding sites. Magnetite present in some species.	No evidence.
Marine mammals	Magnetic fields used for long distance migration and mapping. Magnetite reported in some species. Sensitive to geomagnetic minima that are correlated to strandings.	One species of dolphin uses specialized cells not found in other species.

#### 4.2.2 EMF literature 2017-2019

Table 4.6 gives an overview of recent papers (2017-2019) describing potential impacts of EMFs on marine ecosystems.

Table 4.6: Recent papers, published in 2017-2019.

Year + source	Species	Method	Results of the study
2017a Love et al.	Dungeness crab ( <i>Metacarcinus magister</i> ) and red rock crab ( <i>Cancer productus</i> )	A two-choice bait-experiment was performed using a cage placed on buried and unburied cables. Crabs were given a choice of walking over an energized power cable to a baited trap or walking directly away from that cable to a second baited trap.  The experiment was conducted at two locations, the measured EMF levels were between 13.8 and 116.8 $\mu\text{T}$ in the Santa Barbara Channel and between 24.6 and 42.8 $\mu\text{T}$ at the San Juan Island.	<ul style="list-style-type: none"> <li>There was no evidence that EMF either attracted or repelled crabs.</li> <li>No evidence that the EMF emitted by energized submarine power cables influenced the catchability of these two species of commercially important crabs.</li> <li>No difference in the crabs' responses to lightly buried versus unburied cables.</li> </ul>
2017b Love et al.	Natural occurring fish and invertebrate communities of 44 and 19 different species respectively.	Scuba diving along sections of cables (average EMF levels 73.0 $\mu\text{T}$ - 91.4 $\mu\text{T}$ ), a pipe (average = 0.5 $\mu\text{T}$ ) or sand (0 $\mu\text{T}$ ).	<ul style="list-style-type: none"> <li>No difference in fish and invertebrate communities, any observed differences are likely due to differences in habitat structure.</li> </ul>
2017c Love et al.	Natural occurring fish and invertebrate communities of 41 and 43 different species respectively.	Video recordings with divers and submarines of transects along energized and unenergized power cables, and natural sea floor. Additionally EMF determination by a 3-Axis ELF AC Milligauss Meter and EMF levels approached background levels at one meter distance from the cable. EMF levels were $107.6 \pm 36.6 \mu\text{T}$ (microtesla) at 0 m distance from the cable.	<ul style="list-style-type: none"> <li>Fish communities at energized an unenergized cables were not statistically differing, however fish density around cables was higher compared to natural habitats.</li> <li>Invertebrate biodiversity and density was higher around cables compared to the natural environment.</li> <li>Higher invertebrate and fish abundances are likely the result of an increased complexity of the habitat (e.g. more hard substrate).</li> </ul>



2018 Scott et al.	Edible crab, <i>Cancer pagurus</i>	Crabs were kept in 1000 L flow through tanks and stress related parameters were measured (L-Lactate, D-Glucose, Haemocyanin and respiration rate) along with behavioral and response parameters (antennular flicking, activity level, attraction/avoidance, shelter preference and time spent resting/roaming) during 24-h periods of simulated EMF. The experiments were carried out by two EMF peak values, 40mT and 2.8 mT.	<ul style="list-style-type: none"> <li>EMFs will likely affect edible crabs both behaviorally and physiologically. Exposure to EMF had no effect on Haemocyanin concentrations, respiration rate, activity level or antennular flicking rate.</li> <li>EMF exposure significantly disrupted haemolymph L-Lactate and D-Glucose natural circadian rhythms.</li> <li>Crabs showed a clear attraction to EMF exposed shelter (69%) compared to control shelter (9%) and significantly reduced their time spent roaming by 21%.</li> </ul>
2018 Wyman et al.	Late-fall run Chinook salmon ( <i>Oncorhynchus tshawytscha</i> )	Detection salmon records of tagged salmon smolts were analyzed during their out-migration through the San Francisco Bay before and after the installation of an 85-km high-voltage direct-current transmission cable. The cable had a modelled mean MF anomaly of $543 \pm 34$ nT and $185 \pm 12$ nT at heights of 5 and 10m above the bottom.	<ul style="list-style-type: none"> <li>Cable activity appeared to have mixed, but limited effects on movements and migration success of salmon smelts.</li> <li>After cable energization, higher proportions of fish crossed the cable location and fish were more likely to be detected south of their normal migration route.</li> <li>Cable activity did not significantly impact the proportion of fish that successfully migrated through the bay or the probability of successful migration.</li> </ul>
2018 Hutchinson et al.	American lobster, <i>Homarus americanus</i> and Little skate, <i>Leucoraja erinacea</i> <sup>[SEP]</sup>	Field survey to determine EMF levels from high voltage direct current (HVDC) cables (the CSC and Neptunus cable) and one AC cable. The DC magnetic fields measured deviated from the background magnetic field in the range of 0.4-18.7 $\mu$ T for the CSC and 1.3-20.7 $\mu$ T for the Neptune Cable. The maximum observed AC values along the cable axis were 0.15 $\mu$ T. Behavioural experiments using large netted enclosures with tagged lobsters and skates were performed.	<ul style="list-style-type: none"> <li>DC and AC magnetic fields extended out to 5 and 10 m from either side of the cables respectively, whereas the AC electric fields (from a nearby transformer) extended out to 100 m from either side of the cable.</li> <li>American lobster exhibited a statistically significant but subtle change in behavioral activity (closer to the seabed and more turns) when exposed to the EMF of the HVDC cable,</li> <li>Little skate exhibited a strong behavioral response to the EMF from the CSC; they showed more exploratory activity and spend more time in the zone of high EMF.</li> <li>The EMF associated with the CSC did not constitute a barrier to movements across the cable for either lobsters or skates.</li> </ul>
2019 Hutchinson et al.	American Eel <i>Anguilla rostrata</i>	Telemetry study of tagged eels in an area with an HVDC cable (see Hutchinson et al. 2018) where EMFs (47-53.3 $\mu$ T) were simultaneously measured in situ.	<ul style="list-style-type: none"> <li>Of 12 eels with high quality tracks 10 crossed the cable, with 6 crossing more than once.</li> <li>Behavioural responses not yet analysed, study will be repeated.</li> </ul>

Additionally several review papers were published recently focusing on the impact of power cables in general. Biasotto et al. (2018) concluded that most negative impacts appear during the construction of power cables. Looking into the impact of EMFs specifically, they found both negative and positive impacts on ecology. Furthermore, Taormina et al. (2018) reviewed the potential impacts of power cables on the marine environment during the different phases of operation, installation and decommissioning.

They made a diagram of potential impacts caused by different types of submarine cables (Figure 4.8) and summarized all impacts in a table (Table 4.6). Moreover, they concluded that the main potential impacts of power cables are associated with EMFs, the creation of reefs and 'reserve' effects, since human activity is often forbidden in an area with submarine power cables.

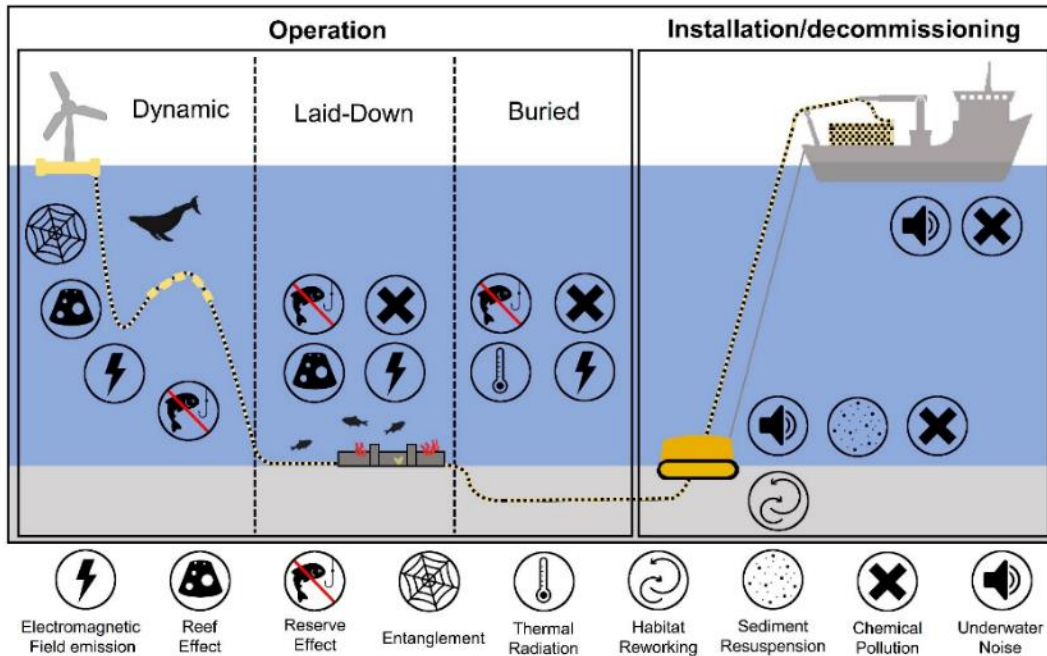


Figure 4.8: Potential impacts of power cables on the marine environment, during operation, installation and decommissioning (from: Taormina et al. 2018).

Table 4.6: Potential impacts, and extent of impact, of power cables on the marine environment, during installation, decommissioning and maintenance (top) and during operation (bottom) on different marine compartments. LD = Laid-down, Dyn = Dynamic and black fill = no impact (from: Taormina et al. 2018).

	Physical habitat			Invertebrates			Fish			Elasmobranch and Diadromous Fish			Marine mammals		
<b>Installation / Decommissioning / Maintenance</b>															
	Bur	LD	Dyn	Bur	LD	Dyn	Bur	LD	Dyn	Bur	LD	Dyn	Bur	LD	Dyn
Seabed disturbance	①	①		①	①		②	①							
Sediment resuspension	①			①	①		①	①		①	①				
Chemical pollution				①	①	①	①	①	①	①	①	①	①	①	①
Underwater noise				②	②	②	①	①	①	①	①	①	①	①	①
<b>Operation</b>															
	Bur	LD	Dyn	Bur	LD	Dyn	Bur	LD	Dyn	Bur	LD	Dyn	Bur	LD	Dyn
Reef effect		①	②		①	②		①	②		①	②			
Reserve effect	①	①	①	①	①	①	①	①	①	①	①	①	①	①	①
Chemical pollution				①	①	①	①	①	①	①	①	①	①	①	①
Electromagnetic fields				③	③	③	②	②	③	②	②	③			②
Heat emission				②	①	①									
Entanglement									②			②			②

Extent of impact	Negligible	Low	Medium	High
Uncertainty	① Low	② Medium	③ High	



# 5 CONCLUSION

The overall objective of the project was to reduce assumptions regarding EMF and gather empirical data to increase our understanding of EMF and related effects on organisms.

Therefore, it was aimed to develop a monitoring methodology to obtain values of generated EMF combined with video observations above the export cables. Below the conclusions on the development of the monitoring methodology, measured EMF strengths and marine life observations are given.

## 5.1 METHODOLOGY

The developed measurement sledge equipped with real-time and submersible EMF sensors proved to be able to measure the EMFs produced by the subsea power cables. The sensors were able to precisely measure the increase in EMF strength while approaching the power cable. With this methodology, all power cables were accurately detected and it was possible to position the measurement sledge – with certainty - directly above the cable.

This field study also shows that the sledge that measures both EMF and benthic fauna at the same time is an effective device that can help detect patterns of marine life around cables. Images were of sufficient quality, in 70-90% of the time benthic fauna, both mobile and epifauna species, could be detected and subsequently related to the measured EMF strengths. This allowed the gathering of information on the presence of marine life directly above the subsea power cables, which are under influence of EMFs.

A limitation of the developed methodology was the use of a small survey vessel in relation to the wind conditions. A small vessel was chosen to prevent disturbance from (electrical) equipment and a steel hull on the EMF measurements. However, as a result, measurements could only be conducted during very low wind conditions. This resulted in a limited dataset that was insufficient to use for model validation.

## 5.2 EMF MEASUREMENTS

An increase of the EMF was measured directly above each cable. The measured EMF values were relatively low due to the fact that measurements were only conducted during low wind speeds, which implied that power production (and hence current) from the OWFs was limited.

Differences in measured EMF values could due to the limited dataset not directly be explained by the factors influencing the EMF strength, though the relation between power and EMF strength was demonstrated.

All three wind park cables generated EMF values of low magnitude in the range of tenths of microtesla, 0.036  $\mu$ T to 0.072  $\mu$ T.

Under the measured conditions, a zone with increased EMF values in comparison to the background values between 7.5m and 24.5m horizontal distance on both sides of the cables was determined. This zone is expected to be larger under high wind conditions due to the increase of the EMF value with power production.



### 5.3 MARINE LIFE

Based on a single observation at PAWP cable at 4-6-2019, it has been observed for at least two species groups that there is a difference in the density, directly above the cable (in areas with high EMF values), compared to areas further away from the cable (low EMF values). Considering that this is only a single observation and no repeated quantitatively research and analysis could be conducted, no firm conclusions could be drawn from the results of this field study.

A review of recently published scientific literature shows that field and experimental studies of EMF effects are still scarce, because EMFs are often not measured in the field. Consequently, results are mixed and based on animal responses rather than changes at population scale. Therefore, it is problematic to evaluate ecologically significant changes and to determine true impact (Taormina et al. 2018; Hutchinson 2018).



# 6 DISCUSSION

## 6.1 MEASUREMENTS OF EMF'S

Measured EMF strength between the different cables were all the same order of magnitude, though clearly higher EMF values were measured on the first day in comparison to the second day.

However, the variation observed between cables and between transects and/or measurement days could not directly be explained by the relevant factors influencing the EMF strength. There could be several reasons for this:

- 1) The number of observations (2 days, 5 cables) is too limited to make a solid assessment.
- 2) Measurements have been carried out during low wind speeds only. This was due to the development of the methodology on the first day, but also with respect to safety issues on the second measurement day. Although more rough conditions were encountered in the morning (wind speed up to 5-6 Bft briefly), the increased waves did not allow us to deploy the measurement sledge safely. Therefore, measurements were briefly postponed to the afternoon, during which lower wind speeds and waves were present. Since the EMF strength increases with current, it is expected that significantly higher EMF strengths are measured if the wind park produces at maximum power (current).

The measured values are lower compared to other studies. This could be well explained by the relatively calm wind conditions during the measurement period. The prevailing wind speeds were not larger than 3-4 Bft on 20-06-2019 and 04-06-2019, respectively. In general, wind parks yield their maximum capacity starting at wind of 6 Bft (EZK, n.d.). The measured EMF – although relatively low - were in a similar magnitude range than found in a model study by Gill et al. (2005) for two standard export cables. The authors modelled an average EMF of 0.01-0.015  $\mu\text{T}$  with maximum values of 0.02-0.03  $\mu\text{T}$  (Gill et al. 2005).

Other studies, such as field measurements of DNVGL showed values varying between 0.125  $\mu\text{T}$  at 2 m distance to 3.2  $\mu\text{T}$  and 6.54  $\mu\text{T}$  at 0.5 m distance for electricity currents of 436 A and 432 A, respectively.

## 6.2 MARINE LIFE

The field of EMF effects and impacts on marine biodiversity is still in its early days and field tests are still rare. Experience with EMF measurements in relation to marine life will lead to increased understanding of method optimization. Based on image analysis at 1 of 4 cable transects a pattern in benthic fauna in relation to EMF strength is suggested. This is the first field result for potential cable effects on marine life in the Netherlands. This pattern was however not repeated, and results are not sufficient to draw firm conclusion.

We began this study with the understanding that if a species is attracted to an EMF we would expect to find that species in disproportionately larger numbers around an energized cable with high EMF strength compared to further away from the cable. Similarly, if a species is repelled by that EMF we would expect that specific species in lower densities close to the cables. However, the presence or absence of an EMF is not the only habitat parameter influencing how an organism chooses its habitat. Presence and absence can be explained by other habitat parameters like topology and sediment characteristics of the sea bed (De Jong et al., 2015), presence of hard substrate (gravel, shell material, reef building species) or seabed temperature due to heating by the cable.



For example, the seabed in the area where the transects were carried out consists predominantly of soft sediment, therefore sediment dynamics and hydrodynamics play an important role in shaping local physical conditions and thus benthos habitat. The habitat characteristics differ between high and low dynamic areas, and between the top and the valley of these sand waves, influencing the occurrence of several benthic species (Damveld et al. 2018) Therefore, the bathymetry of the transects carried out in this study were checked for the occurrence of sand banks and sand waves. Transects of PAWP and LUD were located > 15 meter and in homogeneous areas with small differences in bathymetry. The OWEZ transect was located in an area that is slowly sloping towards shallower depths and 10-15 meters.

Additionally, behaviour could be another possible explanation for the occurrence of patches with high densities of certain species. For instance sea potatoes aggregations formed in the period June, July and August, which is corresponding to their breeding season, has been described in scientific literature (Buchanan, 1966). For future field studies it is recommended to include other explaining factors as well.

One explaining factor for lack of quantitative analyses, is that effects cannot be detected, if benthic species are present in low abundances only. Increasing the amount of transects and data and thereby specifically aiming for locations with sufficient abundance of mobile fauna and benthic species will improve the method. An option would be to first select a location with high benthic abundance based on images only (e.g. using a drop cam). Measuring EMF transects perpendicular to the cable at these sites will yield more robust results.

It is at least recommended to collect images when measuring EMF fields in the future, because this will lead to more data that can be processed in a later point in time and will help to improve method optimization.

### 6.3 CURRENT KNOWLEDGE ON POTENTIAL IMPACT OF EMFs

The first underwater power cable was laid down in 1811 in Germany (Taormina et al. 2018) and since then a large expansion of submarine cables took place. Especially with the growth of energy consumption and energy at sea developments, the area with EMFs is expanding rapidly and especially the electric power transmitted through cables is increasing rapidly.

In recent years the attention for the impact of EMFs is increasing. However, field studies considering the impact of EMFs on marine animals are still rare. An early mesocosm study showed that the response of several elasmobranch species was not predictable and seemed to be species, or even individual, specific (Gill et al. 2009). Due to these mixing results, it is hard to draw conclusions.

Recent field studies do again show contrasting findings: fish and invertebrate communities do not statistically differ with areas with varying EMFs. The density can be higher near cables (Love et al. 2017b, 2017c), but this is hypothesized to be explained by habitat structure difference (addition of hard substrate). EMFs have a behavioural effect on edible crabs, little skates and American lobsters (Scott et al. 2018, Hutchison et al. 2018), but mixed and limited effects on smolts (Wyman et al. 2018) and no effect on Dungeness and red rock crabs (Love et al. 2017a). Based on these studies, there is no evidence of a barrier effect of EMFs associated with cables to animal movement since in all experimental or field studies EMFs did not prevent species to cross the cables. While the experimental studies conducted recently provide clear evidence of a behavioural response when receptive animals encountered the EMF (Scott et al. 2018, Hutchison et al. 2018), the evidence for a biological impact is to date assessed as minor.

## 6.4 RECOMMENDATIONS

The following recommendations are made:

### EMF measurements / cable configuration

- With the developed methodology, we recommend to further study the presence of EMFs by subsea power cables and its potential impact on marine life.
- We recommend to assess the disturbance of larger vessels on the EMF measurements, as in case the influence is limited this would allow for measurements during higher wind conditions.
- In this study, only export cables to shore have been measured. We recommend to measure also infield cables inside the wind farm.
- Since measurements have been conducted during relatively calm weather, we recommend to conduct continuous measurements of EMF under varying wind conditions up to maximum power production.
- It is recommended to conduct long term measurements either by a stand-alone system placed at the sea bottom above varying burial depths, combined with video cameras. Long term measurements can also be conducted at the beach where the cable comes to shore, this ensures safe measurements during high-wind periods as well.
- More detailed information on cable types and characteristics of each export cable can help explaining variations in measured EMF. It is therefore recommended to include manufacturers / TenneT in future research on EMFs of subsea power cables.
- In this study, EMFs of AC export cables have been measured. Although the currently planned export cables will also consist of AC cables, it is recommended to start studying the EMFs of DC cables as well. There are currently already DC cables present in the Dutch coastal zone (BritNed, NorNed & Cobra cable) and for future development of offshore wind farms further offshore also DC export cables are expected.

### Model validation

- We recommend validating the EMF models used for the prediction of EMF strengths under the various wind conditions (power production) and burial depths (distance from the cable).

### Ecology

- Two days of field measurements have provided valuable insights in the megafauna above the subsea power cables. Due to the limited amount of data, no hard conclusion on potential impact on marine life can be drawn yet, it is therefore recommended to repeat measurements with more transects.
- It is recommended to further study the role of EMF in relation to habitat selection of marine species.
- It is recommended to further study habitat factors such as D50 and organic matter above cable transects in comparison to the surrounding area, as these could be altered by cable installation or cable presence (e.g. due to EMFs, temperature).
- It is recommended to further study behavioural effects of key North Sea species (both benthos and other species groups such as Elasmobranchs, migratory fish and marine mammals) related to EMFs, including dose-response relations at realistic EMF levels and evaluation of ecologically significant changes.



## 7 REFERENCES

- Biasotto, L. D., & Kindel, A. (2018). Power lines and impacts on biodiversity: A systematic review. *Environmental Impact Assessment Review*, 71, 110-119.
- Buchanan, J.B., 1966. The biology of *Echinocardium cordatum* (Echinodermata: Spatangoidea) from different habitats. *Journal of the Marine Biological Association of the United Kingdom*, 46, 97-114
- CMACS. 2003. "A Baseline Assessment of Electromagnetic Field Generated by Offshore Windfarm Cables." Offshore (Conroe, TX): 66.
- Damveld, J. H., van der Reijden, K. J., Cheng, C., Koop, L., Haaksma, L. R., Walsh, C. A. J., et al. (2018). Video transects reveal that tidal sand waves affect the spatial distribution of benthic organisms and sand ripples. *Geophysical Research Letters*, 45, 11,837–11,846. <https://doi.org/10.1029/2018GL079858>.
- De Jong M. F., M. J. Baptist, H. J. Lindeboom, P. Hoekstra. 2015. Relationships between macrozoobenthos and habitat characteristics in an intensively used area of the Dutch coastal zone. *ICES Journal of Marine Science* 2409–2422 72 (8), 2409–2422
- DNV-GL, 2015. Magneetvelden Exportkabel PAWP. Meting en berekening magnetische veldsterkten. Rapport nr.: 16-0144 v2a
- Gill, A.B., I Gloyne-Phillips, K.J. Neal, and J.A. Kimber. 2005. COWRIE 1.5 Electromagnetic Fields Review - The Potential Effects of Electromagnetic Fields Generated by Sub-Sea Power Cables Associated with Offshore Wind Farm Developments on Electrically and Magnetically Sensitive Marine Organisms – a Review.
- Gill, A., Huang, Y., Gloyne-Phillips, I., Metcalfe, J., Quayle, V., Spencer, J., & Wearmouth, V. C. (2009). 2.0 Electromagnetic Fields (EMF) Phase 2: EMF-sensitive fish response to EM emissions from sub-sea electricity cables of the type used by the offshore renewable energy industry. Report by Centre for Environment Fisheries and Aquaculture Science (CEFAS), Centre for Intelligent Monitoring Systems (CIMS), Centre for Marine and Coastal Studies Ltd (CMACS), Cranfield University, and University of Liverpool, 128.
- Hutchison, Z., Sigray, P., He, H., Gill, A. B., King, J., & Gibson, C. (2018). Electromagnetic Field (EMF) Impacts on Elasmobranch (shark, rays, and skates) and American Lobster Movement and Migration from Direct Current Cables. Sterling (VA): US Department of the Interior, Bureau of Ocean Energy Management. OCS Study BOEM, 3.
- Hutchison, Z., Gill, A. B., Sigray, P., King, J.W. (2019). An experimental approach to determine if anguillid eels respond to the electromagnetic field of subsea buried cables. Poster, Conference on Wind and Wildlife 2019.
- Love, M. S., Nishimoto, M. M., Clark, S., McCrea, M., & Bull, A. S. (2017a). Assessing potential impacts of energized submarine power cables on crab harvests. *Continental Shelf Research*, 151, 23-29.
- Love, M. S., Nishimoto, M. M., Clark, S., McCrea, M., & Bull, A. S. (2017b). The organisms living around energized submarine power cables, pipe, and natural Sea floor in the inshore waters of Southern California. *Bulletin, Southern California Academy of Sciences*, 116(2), 61-88.
- Love, M. S., Nishimoto, M. M., Snook, L., Schroeder, D. M., & Scarborough Bull, A. (2017c). A Comparison of Fishes and Invertebrates Living in the Vicinity of Energized and Unenergized Submarine Power Cables and Natural Sea Floor off Southern California, USA. *Journal of Renewable Energy*.



- Meyer, Carl G., Kim N. Holland, and Yannis P. Papastamatiou. 2005. "Sharks Can Detect Changes in the Geomagnetic Field." *Journal of the Royal Society Interface* 2(2): 129–30.
- Normandeau, Exponent, T Tricas, and A Gill. 2011. *Energy Effects of EMFs from Undersea Power Cables on Elasmobranchs and Other Marine Species*. Pacific OCS Region, Camarillo, CA.
- Scott, K., Harsanyi, P., & Lyndon, A. R. (2018). Understanding the effects of electromagnetic field emissions from Marine Renewable Energy Devices (MREDs) on the commercially important edible crab, *Cancer pagurus* (L.). *Marine pollution bulletin*, 131, 580-588.
- Snoek, R.C., R. de Swart, K. Didderen, W. Lengkeek, M. Teunis (2016). Potential effects of electromagnetic fields in the Dutch North Sea Phase 1: Desk Study. WP2016\_1031.
- Sutton, Simon J., Paul L. Lewin, and Steve G. Swingler. 2017. "Review of Global HVDC Subsea Cable Projects and the Application of Sea Electrodes." *International Journal of Electrical Power and Energy Systems* 87: 121–35. <http://dx.doi.org/10.1016/j.ijepes.2016.11.009>.
- Taormina, Bastien et al. 2018. "A Review of Potential Impacts of Submarine Power Cables on the Marine Environment: Knowledge Gaps, Recommendations and Future Directions." *Renewable and Sustainable Energy Reviews* 96(July): 380–91. <https://doi.org/10.1016/j.rser.2018.07.026>.
- Taormina, B., Bald, J., Want, A., Thouzeau, G., Lejart, M., Desroy, N., & Carlier, A. (2018). A review of potential impacts of submarine power cables on the marine environment: Knowledge gaps, recommendations and future directions. *Renewable and Sustainable Energy Reviews*, 96, 380-391.
- Wyman, M. T., Klimley, A. P., Battleson, R. D., Agosta, T. V., Chapman, E. D., Haverkamp, P. J., ... & Kavet, R. (2018). Behavioral responses by migrating juvenile salmonids to a subsea high-voltage DC power cable. *Marine biology*, 165(8), 134.


#### **Websites:**

Ministerie van Economische Zaken (EKZ): <https://www.windenergie.nl/windenergie-op-land/feiten-en-cijfers>



# APPENDIX A

## A1. CABLE TYPES



Type	1	2	3	4	5
<b>Rated voltage</b>	33 kV AC	150 kV AC	420 kV AC	320 kV DC	450 kV DC
<b>Insulation</b>	XLPE, EPR	XLPE	Oil/paper or XLPE	Extruded	Mass-impregnated
<b>Typical application</b>	Supplying small islands, connection of offshore wind turbines	Connecting islands with large populations, offshore wind parks export cables	Crossing rivers/straights with large transmission capacity	Long distance connections of offshore platforms or wind farms	Long distance connection of autonomous power grids
<b>Maximum length</b>	20–30 km	70–150 km	<50 km	>500 km	>500 km
<b>Typical rating</b>	30 MW	180 MW	700 MW/three cables	1000 MW/cable pair	600 MW/cable

Figure A. 1: Description of five standard undersea export cables (Photo's: 1-Standard cable; 2, 3, 4-Ningbo Orient Wires and Cables Co. Ltd; 5=ABB Sweden), XLPE: Cross-Linked Polyethylene; EPR: Ethylene Propylene Rubber (extracted from (Taormina et al. 2018)).



# APPENDIX B CALIBRATION CERTIFICATE



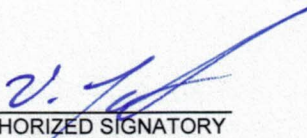
# Calibration Certificate

Narda Safety Test Solutions hereby certifies that the object referenced to this certificate has been calibrated by qualified personnel using Narda's approved procedures. The calibration was carried out in accordance with a certified quality management system which conforms to ISO 9001.

OBJECT	Exposure Level Tester ELT-400
PART NUMBER (P/N)	2304/04
SERIAL NUMBER (S/N)	N-0636
MANUFACTURER	Narda Safety Test Solutions GmbH
CUSTOMER	
CALIBRATION DATE (YYYY-MM-DD)	2017-02-06
RESULT ASSESSMENT	within specifications
AMBIENT CONDITIONS	Temperature: (23 ± 3) °C Relative humidity: (20 to 60) %
CALIBRATION PROCEDURE	2300-8701-00A

ISSUE DATE: 2017-02-06  
(YYYY-MM-DD)

  
CALIBRATED BY

  
AUTHORIZED SIGNATORY

MANAGEMENT  
SYSTEM



This calibration certificate may not be reproduced other than in full except with the permission of the issuing laboratory. Calibration certificates without signature are not valid.

Certified by DQS according to  
ISO 9001:2008  
(Reg.-No. 099379 QM08)

## OBJECT

A complete ELT system is a combination of an ELT basic instrument (P/N 2304/xx) and an isotropic probe (P/N 2300/90.xx).

Since the probe contains a set of coils, an induced voltage proportional to the time derivative of the magnetic flux density is produced. The basic instrument contains an integrating stage to recover the waveform of the magnetic flux density. The instrument also includes ranging amplifiers, band-limiting filters and a detector, separately for each of the three channels (x, y, z). The results are derived as the

resultant magnetic flux density  $B_{act} = \sqrt{B_x^2 + B_y^2 + B_z^2}$ .

In "FIELDSTRENGTH" mode, the basic instrument indicates the resultant magnetic flux density.

In "EXPOSURE" mode, filters are implemented to provide a frequency response that conforms to a standard selected by the user. The instrument indicates "percentage of limit value", i.e.  $pct = B_{act} / B_{lim}$ .

Note: The filters consist of 1<sup>st</sup> order stages providing a smooth shape to the limit curve representing  $B_{lim}$ . If the particular standard defines sharp edges, deviations are unavoidable at the corner frequencies. See operating manual for nominal shapes.

## METHOD OF MEASUREMENT

The basic instrument was calibrated without a probe by direct measurement using the voltage injection technique.

## CALIBRATION PROCEDURE

An AC voltage was applied to the input connector. The voltage was measured using a calibrated digital voltmeter. The three channels (x-, y-, z-axis) were calibrated separately.

The calibration results are given as the relative sensitivity  $RS = X_{act} / X_{nom}$  where  $X_{nom}$  is shown in the table. The nominal value  $X_{nom}$  works together with the response of an ELT probe in order to meet the specifications published in the data sheet of the ELT system.

- **Frequency Response**

Each of the four operating modes shares a number of functional units with other modes. Calibration was performed using a subset of frequencies and levels for each mode and each range. The entire frequency range was covered by the combination of all these subsets.

Voltage levels and frequencies were set accordingly to generate an indication close to four times the nominal measurement range.

- **Noise Level**

The RMS value of the intrinsic noise level was calibrated with no signal applied.

- **Scope Output**

The relative sensitivity at the analog output was calibrated as the ratio of output to input voltage.

- **Miscellaneous**

More parameters are individually calibrated but not printed in this certificate:

- Gain of the high pass filters (LOW CUT)
- Gain of the range switches (RANGE)
- Linearity of the analog to digital converter (ADC)

## METROLOGICAL TRACEABILITY

The calibration results are traceable to the International System of Units (SI) in accordance with ISO/IEC 17025. The measuring equipment used for calibration is traceable through the reference standards listed below.

STANDARD	MANUFACTURER	MODEL	SERIAL NUMBER	CERTIFICATE	NEXT CAL. DATE	TRACE
Waveform Generator	Agilent	33120A	MY40017646	MMID-00751-20150424	2017-04	in-house
# <i>Frequency Counter</i>	<i>Advantest</i>	R5362B	<i>120700137</i>	<i>306115 D-K-15012-01-00 2014-03</i>	<i>2016-03</i>	<i>DAkKS</i>
Digital Multimeter	Agilent	3458A	US28029061	1-8374074743-1	2017-12	UKAS 0147

# Reference standard (*in italics*) used for in-house calibration of the working standard listed in the line above

## UNCERTAINTY

The reported expanded uncertainty U is based on a standard uncertainty multiplied by a coverage factor  $k = 1.96$ , providing a level of confidence of approximately 95 %. The uncertainty evaluation has been carried out in accordance with the "Guide to the Expression of Uncertainty in Measurement" (GUM).

The reported uncertainty is derived from the uncertainty of the calibration procedure and the object during calibration, and makes no allowance for drift or operation under other environmental conditions.

## MEASURING CONDITIONS

The calibration was performed using a continuous wave signal (CW) and with the indication of the object 20 dB above noise level.

## RESULTS

### Frequency Response – MODE 1: IEC 62233

DETECT: RMS – RANGE: High – LOW CUT: 1Hz

$f$ kHz	$X_{nom}$ %/V	$RS$			$U$ %
		x-axis	y-axis	z-axis	
0.001	708.96	1.0345	1.0292	1.0432	0.047
0.002	1 797.80	1.0147	1.0147	1.0169	0.047
0.010	6 289.76	1.0137	1.0142	1.0129	0.047
0.050	7 965.25	1.0030	1.0025	1.0018	0.027
0.400	7 228.60	1.0037	1.0017	1.0022	0.027
1.000	5 049.64	1.0058	1.0010	1.0043	0.027
10.000	646.22	1.0081	1.0009	1.0069	0.034

DETECT: RMS – RANGE: Low – LOW CUT: 1Hz

$f$ kHz	$X_{nom}$ %/V	$RS$			$U$ %
		x-axis	y-axis	z-axis	
120.000	71.71	1.0082	1.0037	1.0062	0.4
320.000	61.74	1.0095	1.0108	1.0045	1.1
400.000	53.56	0.9945	0.9960	0.9977	1.1
800.000	6.16	0.9423	0.9386	0.9575	1.1



**Frequency Response – MODE 2: ICNIRP 1998 occupational**  
 DETECT: RMS – RANGE: High – LOW CUT: 1Hz

$f$ kHz	$X_{nom}$ %N	RS			U %
		x-axis	y-axis	z-axis	
0.001	141.79	1.0568	1.0518	1.0650	0.047
0.002	359.56	1.0358	1.0363	1.0386	0.047
0.010	1 257.96	1.0157	1.0164	1.0154	0.047
0.050	1 593.16	1.0057	1.0052	1.0047	0.027
0.400	1 450.81	1.0041	1.0051	1.0039	0.027
1.000	1 020.94	1.0018	1.0063	1.0028	0.027
10.000	132.78	1.0004	1.0079	1.0024	0.034

DETECT: RMS – RANGE: Low – LOW CUT: 1Hz

$f$ kHz	$X_{nom}$ %N	RS			U %
		x-axis	y-axis	z-axis	
120.000	23.72	1.0056	1.0069	1.0049	0.4
320.000	26.33	1.0110	1.0130	1.0063	1.1
400.000	23.43	0.9955	0.9973	0.9988	1.1

**Frequency Response – MODE 3: 320  $\mu$ T**

DETECT: RMS – RANGE: High – LOW CUT: 1Hz

$f$ kHz	$X_{nom}$ TV	RS			$U$ %
		x-axis	y-axis	z-axis	
0.400	1.01m	1.0094	1.0071	1.0031	0.027
1.000	404.17 $\mu$	1.0072	1.0071	1.0030	0.027
10.000	40.42 $\mu$	1.0103	1.0113	1.0073	0.034

DETECT: RMS – RANGE: Low – LOW CUT: 1Hz

$f$ kHz	$X_{nom}$ TV	RS			$U$ %
		x-axis	y-axis	z-axis	
120.000	3.47 $\mu$	1.0134	1.0127	1.0140	0.4
320.000	1.61 $\mu$	1.0197	1.0285	1.0202	1.1
400.000	1.16 $\mu$	1.0063	1.0089	1.0248	1.1

**Frequency Response – MODE 4: 80 mT**

DETECT: RMS – RANGE: High – LOW CUT: 1Hz

$f$ kHz	$X_{nom}$ TV	RS			$U$ %
		x-axis	y-axis	z-axis	
0.001	285.79m	1.0153	0.9793	0.9953	0.047
0.002	185.31m	0.9943	0.9893	0.9903	0.047
0.010	40.28m	1.0059	1.0029	1.0039	0.047
0.050	8.08m	1.0080	1.0050	1.0060	0.027

**Noise Level**

DETECT: RMS –LOW CUT: 1 Hz

MODE	Range	
	LOW	HIGH
IEC 62233	0.2732%	1.0909%
ICNIRP 1998 occupational	0.1462%	1.0956%
320 $\mu$ T	254.1877nT	350.0614nT
80 mT	9.5458 $\mu$ T	55.7137 $\mu$ T

DETECT: RMS – LOW CUT: 10 Hz

MODE	Range	
	LOW	HIGH
IEC 62233	0.2794%	1.1198%
ICNIRP 1998 occupational	0.1577%	1.1019%
320 $\mu$ T	45.3680nT	222.9756nT
80 mT	7.6636 $\mu$ T	55.2650 $\mu$ T

DETECT: RMS – LOW CUT: 30 Hz

MODE	Range	
	LOW	HIGH
IEC 62233	0.2760%	1.1271%
ICNIRP 1998 occupational	0.1526%	1.1054%
320 $\mu$ T	35.7030nT	222.8627nT
80 mT	7.4520 $\mu$ T	55.5463 $\mu$ T

**Scope Output (analog)**

MODE 1 (see page 4) – RANGE: LOW – LOW CUT: 1Hz

$f$ Hz	$X_{nom}$ V/V	$RS$			$U$ %
		x-axis	y-axis	z-axis	
400	3.61	1.00117	1.00052	1.00047	0.038

**INTERPRETATION**

The worst-case uncertainty of the object was calculated from the calibration results reported in the "Frequency Response" sections using commonly accepted statistical rules.

MODE	worst-case uncertainty $U_{meter}$		
	1 Hz to 10 Hz	10 Hz to 120 kHz	120 kHz to 400 kHz
Any mode	12.5 %	2.1 %	3.9 %

Note: The uncertainty results for the object settings LOW CUT: 10 Hz and LOW CUT: 30 Hz are valid above 100 Hz and 300 Hz, respectively.

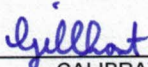
The total uncertainty of the system shall be calculated using  $U_{system} = \sqrt{U_{meter}^2 + U_{probe}^2}$

# Calibration Certificate

Narda Safety Test Solutions hereby certifies that the object referenced to this certificate has been calibrated by qualified personnel using Narda's approved procedures. The calibration was carried out in accordance with a certified quality management system which conformed to ISO 9001.

OBJECT	B- Field Probe 100 cm <sup>2</sup>
PART NUMBER (P/N)	2300/90.10
SERIAL NUMBER (S/N)	M-1111
MANUFACTURER	Narda Safety Test Solutions GmbH
CUSTOMER	
CALIBRATION DATE (YYYY-MM-DD)	2017-02-16
RESULT ASSESSMENT	within specifications
AMBIENT CONDITIONS	Temperature: (23 ± 3) °C Relative humidity: (20 to 60) %
CALIBRATION PROCEDURE	2300-8701-00A

ISSUE DATE: 2017-02-16  
(YYYY-MM-DD)

  
CALIBRATED BY

  
AUTHORIZED SIGNATORY

MANAGEMENT  
SYSTEM



This calibration certificate may not be reproduced other than in full except with the permission of the issuing laboratory. Calibration certificates without signature are not valid.

Certified by DQS according to  
ISO 9001:2008  
(Reg.-No. 099379 QM08)

## OBJECT

A complete ELT system comprises of an ELT basic unit (P/N 2304/xx) and an isotropic probe (P/N 2300/90.xx).

The probe consists of three coils of wire in an orthogonal arrangement. The object produces induced voltages proportional to the time derivative of the magnetic field. This air-core probe does not include active components, i.e. it is linear up to high field levels. The cross-sectional area of the coils is 100 cm<sup>2</sup> (P/N 2300/90.10) and 3 cm<sup>2</sup> (P/N 2300/90.20), respectively.

## METHOD OF MEASUREMENT

The probe was calibrated using the direct measurement method based on calculated flux density.

## CALIBRATION PROCEDURE

During calibration the probe's center coincided with the center of a set of Helmholtz coils. The object was aligned for maximum interception of the applied field, i.e. the handle was oriented 54.7 deg to the vertical B-field. The object was rotated about the axis of the handle by 60° and then stopped to record the indication for each frequency. At every 120° position one axis was aligned with the incident field vector while the other axes were successively cross-polarized.

The output voltage of the object was measured using a specific Exposure Level Tester as a working standard.

The probe's actual efficiency was calculated from the output voltage of the probe divided by the applied magnetic flux density using  $X_{act} = U_{out} / B_x$ . The calibration results are given as the relative sensitivity  $RS = X_{act} / X_{nom}$  where  $X_{nom}$  is shown in the table. The nominal value  $X_{nom}$  works together with the response of an ELT basic unit in order to meet the specifications published in the data sheet of the ELT system.

## FIELD GENERATION SETUP

A set of circular "Helmholtz coils" was used generating a nearly uniform, sinusoidal magnetic field. The magnetic flux density was calculated from the coil dimensions, the number of turns in the coils, and the current in the coils. The current was derived from a voltage measured across a shunt:

$$B_x = \mu_0 \cdot \frac{N \cdot r^2}{(r^2 + a^2)^{3/2}} \cdot \frac{U}{R}$$

where...

- $B_x$  is the axial magnetic flux density
- $N$  is the number of turns on each coil ( $N = 1$ )
- $r$  is the radius of each coil (nominal  $r = 0.33$  m)
- $2a$  is the spacing of the coils (nominal  $2a = 0.33$  m)
- $R$  is the resistance of a shunt (nominal  $R = 1$  Ohm)
- $U$  is the voltage measured across the shunt

Reference: IEC 61786 and IEEE 1309

The size of the set of Helmholtz coils had been optimized for a low deviation of the field from the central value. The variation was calculated to be at most 0.1 % over the cross-sectional area of the probe.

The shunt was integrated as part of the coil set.

## METROLOGICAL TRACEABILITY

The calibration results are traceable to the International System of Units (SI) in accordance with ISO/IEC 17025. The measuring equipment used for calibration is traceable through the reference standards listed below.

STANDARD	MANUFACTURER	MODEL	SERIAL NUMBER	CERTIFICATE	NEXT CAL. DATE	TRACE
Waveform Generator	Agilent	33120A	MY40017646	MMID-00751-20150424	2017-04	in-house
# <i>Frequency Counter</i>	<i>Advantest</i>	R5362B	120700137	306115 D-K-15012-01-00 2014-03	2016-03	DAkKS
Exposure Level Tester	Narda	ELT-400	05-EU03	2304GD-05EU03-20161019-6632	2017-10	in-house
# <i>Digital Multimeter</i>	<i>Agilent</i>	3458A	US28029061	1-7514145317-1	2016-12	UKAS 0147
Helmholtz Coil, with integral Shunt	Narda	HHC-332/1	---	MMID-00841-20170120	2019-01	in-house
# <i>Digital Multimeter</i>	<i>Agilent</i>	3458A	US28029061	1-8374074743-1	2017-12	UKAS 0147
# <i>Calliper</i>	<i>Preisser</i>	0223703	310121016	14104161 D-K-15181-01-00 2014-02	2017-02	DAkKS
Digital Multimeter	Agilent	3458A	US28029061	1-8374074743-1	2017-12	UKAS 0147

# Reference standard (*in italics*) used for in-house calibration of the working standard listed in the line above; not used for routine calibration

## UNCERTAINTY

The reported expanded uncertainty  $U$  is based on a standard uncertainty multiplied by a coverage factor  $k = 1.96$ , providing a level of confidence of approximately 95 %. The uncertainty evaluation has been carried out in accordance with the "Guide to the Expression of Uncertainty in Measurement" (GUM). The reported measurement uncertainty is derived from the uncertainty of the calibration procedure and the object during calibration, and makes no allowance for drift or operation under other environmental conditions.

## MEASURING CONDITIONS

The calibration was performed using a continuous wave signal (CW). The magnetic flux density was set to nominal 2.5  $\mu\text{T}$  and with the indication of the object was at least 20 dB above noise level.

## RESULTS

### Frequency Response

$f$ kHz	$X_{nom}$ V/T	RS						$U$ %
		Pos. Y	Pos. YZ	Pos. Z	Pos. ZX	Pos. X	Pos. XY	
0,05	123.71	0.9896	0.9876	0.9819	0.9870	0.9948	0.9928	0.29
0,4	989.68	0.9965	0.9906	0.9938	0.9905	0.9921	1.0009	0.29
30	74.10k	0.9946	0.9896	0.9932	0.9914	0.9915	0.9988	0.57
120	287.87k	0.9921	0.9929	1.0007	0.9998	1.0003	1.0015	0.62
400	611.65k	1.0145	1.0076	1.0058	1.0146	1.0128	1.0122	1.86

## INTERPRETATION

The worst-case uncertainty of the object was calculated from the calibration results reported in the "Frequency Response" section using commonly accepted statistical rules.

Frequency Range	worst-case uncertainty $U_{probe}$
1 Hz to 120 kHz	2.10 %
120 kHz to 400 kHz	2.69 %

Note: As the object is purely a coil the function is not restricted at low frequencies.

The total uncertainty of the system shall be calculated using  $U_{system} = \sqrt{U_{meter}^2 + U_{probe}^2}$